RSC Sustainability

ROYAL SOCIETY OF CHEMISTRY

CRITICAL REVIEW

View Article Online
View Journal | View Issue

Check for updates

Cite this: *RSC Sustainability*, 2023, **1**, 1634

Covalent organic framework-based lamellar membranes for water desalination applications

Akbar Ali,†[ab] Muzmil Thebo,†[c] Dahar Janwary,[g] Muzaffar Iqbal,[d] Waqas Mughal,[e] Jun Yang *[ab] and Khalid Hussain Thebo *[bf]

Received 29th June 2023
Accepted 20th August 2023

DOI: 10.1039/d3su00212h

rsc.li/rscsus

Covalent Organic Framework (COF)-based two-dimensional materials have great potential to be utilized as separation membranes with high permeability and rejection while mitigating the permeability–selectivity trade-off due to their single layer thickness and large specific surface area. This review summarizes the current preparation methods of COF-based membranes, and discusses modification strategies for their physicochemical properties. It also provides an overview of their applications in desalination of seawater, brackish water, and industrial wastewater. Then, we highlight the current engineering hurdles and suggest suitable solutions. Finally, the review focuses on the future research direction to improve the separation performance of existing COF-based membranes.

Sustainability spotlight

Water is an essential resource for human health, economic prosperity, and agricultural output. Globally, billions of people lack access to clean water. As the earth's temperature rises and its population grows, all of these problems are intensifying. Therefore, water scarcity is a crucial issue for both emerging and established nations. In this regard, various purification methods have been studied to solve the problem. Recently, two-dimensional covalent organic frameworks (COFs) have offered high-performance separation membranes for water desalination, pervaporation, and solvent/water separation due to their hydrophilic surface, high mechanical and chemical stability, and flexibility. This review summarizes the current fabrication methods of COF-based lamellar membranes and discusses their applications in water desalination.

1. Introduction

Membrane technology has become one of the promising approaches in various separation and purification processes in wastewater treatment,[1,2] biomedical science,[3] energy conversion,[4] gas-phase separation,[5] fuel cells,[6–9] and pervaporation.[10–12] It has several advantages, such as low energy consumption, small footprint, and simple operation over other conventional technologies. The separation performance of a membrane mainly depends on its material, pore structures and physicochemical properties. Therefore, various organic and inorganic materials *e.g.* porous materials,[13,14] carbon nanotubes,[15–18] functional polymers,[19,20] graphene,[21,22] reduced GO[23,24] *etc.* have been investigating to improve the microstructural and separation properties of membranes. In addition, the cost of the material and membrane is also a big issue for commercialization. So, it is still more challenging to fabricate cost-effective membranes with precisely controlled structure and better permeability, selectivity and stability. Therefore, demand for membranes with extraordinary properties remains a need of membrane industries.

Recently, numerous layered materials, such as graphene,[25–27] metal–organic frameworks,[28,29] transition metal dichalcogenides,[28,30] zeolite,[31,32] hexagonal boron nitride,[33,34] transition metal carbides,[35,36] layered double hydroxides,[37,38] and COFs,[39–43] with monatomic thickness and other distinct characteristics have been developed. They have great capacity to enhance the performance of current technologies due to their outstanding thermal and electrical conductivity, superior mechanical stiffness, strength, and flexibility, high intrinsic carrier mobility, and large specific surface area. In addition, their customizable physicochemical characteristics, in-plane pore structure, and inter-layer 2D channels play a vital role in the development of high-performance membranes. Among them, COFs have attracted significant attention for a variety of applications. Since their discovery in 2005,[44] COFs have become a new member of

[a]State Key Laboratory of Multi-phase Complex Systems, Institute of Process Engineering (IPE), Chinese Academy of Sciences, Beijing 100F190, China. E-mail: jyang@ipe.ac.cn

[b]University of the Chinese Academy of Sciences, 19A Yuquan Road, Beijing 100049, China. E-mail: khalidthebo@yahoo.com

[c]Dr. M. A. Kazi Institute of Chemistry, University of Sindh, Jamshoro 76080, Pakistan

[d]Department of Chemistry, Faculty of Physical and Applied Sciences, The University of Haripur, Haripur 22620, KPK, Pakistan

[e]Department of Mechanical Engineering, Quaid-E-Awam University of Engineering, Science, and Technology, Nawabshah, Sindh, Pakistan

[f]Institute of Metal Research, Chinese Academy of Sciences, Shenyang 110016, China

[g]National Centre of Excellence in Analytical Chemistry, University of Sindh, Jamshoro 76080, Pakistan

† Akbar Ali and Muzmil Thebo contributed equally to this work.

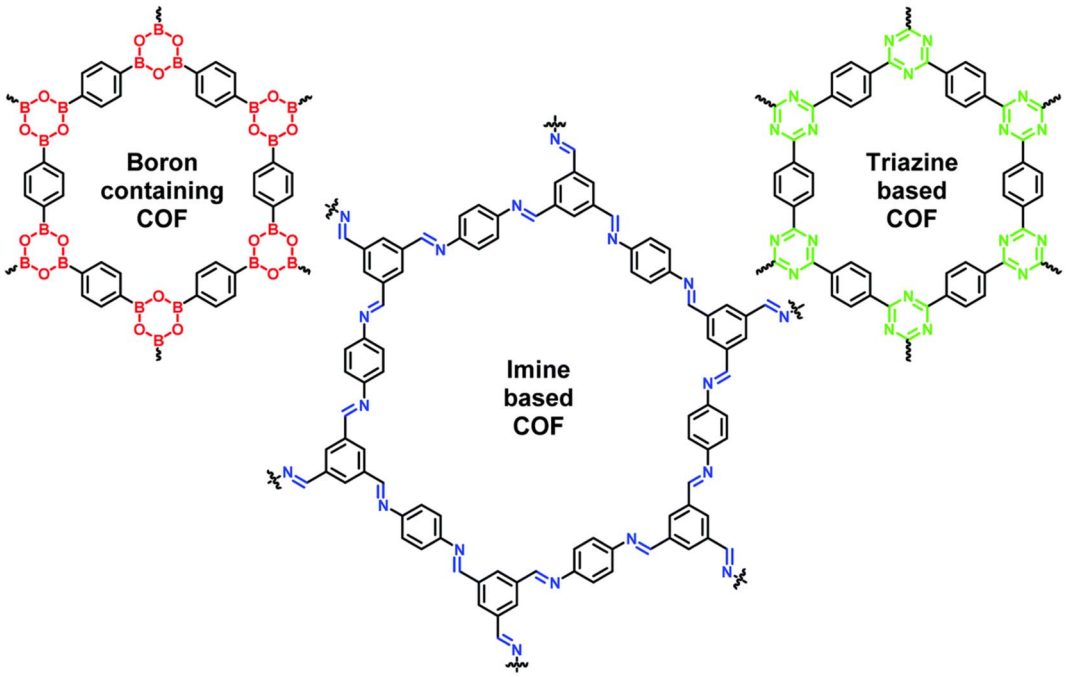

Fig. 1 The common types of COFs and their structures *i.e.* boron-, imine- and triazine-based COFs. Data obtained with permission.[50] Copyrights 2019, Royal Society of Chemistry.

the family of porous crystalline materials. These are strong covalent polymers made of just pure organic elements, such as B, C, H, N, and O (Fig. 1). The reversible covalent bond formation processes, which are often built with stiff monomers, are what give COFs their crystallinity. COFs have a great ability to exfoliate into single layered as well as multilayered nanosheets with high aspect ratios, intriguing characteristics and have multiple uses in storage, separation, catalysis, *etc.* Recent studies showed that COFs can be an ideal material for next-generation water purification membranes due to their high porosity, uniform aperture, low density, and highly ordered crystalline structure.[45–49] They showed an outstanding separation of dyes, protein, medicinal compounds, and salt ions from water due to the controlled pore diameter of COFs (0.6–10 nm). Several initiatives are adopted in this area each year to use such wonder materials for desalination applications. Fig. 2 demonstrated the yearly significant rise in publications on COF-based membranes for desalination and water filtration. However, it is still a significant challenge to fabricate continuous COF membranes with low cost *via* a simple method.

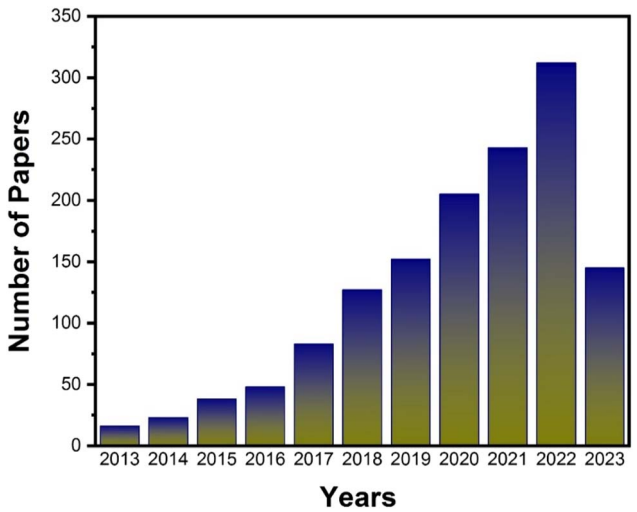

Fig. 2 Number of papers published on COF-based membranes for water desalination and purification per year. Data reproduced from the Web of Science and NIH USA from Jan 2013 to May 2023.

In this review, we focus on the current methods used for the fabrication of COF-based membranes and discuss their advantages and limitations. Further, the effect of modifications on physicochemical properties of membranes will be highlighted. We also discussed the advantages and disadvantages of COF-based membranes for use in desalination and water purification. Finally, we will provide unexplored future avenues for state-of-the-art COF-based membranes. We anticipate that this article will shed further light on the inventive ways that COF materials can be used for exchange and separation applications.

2. Methods of fabrication and physicochemical properties

COFs are an emerging family of 2D porous materials with variable pore sizes, abundance of functional groups, low densities, high specific surface areas, and exceptional chemical and thermal stabilities. Therefore, they can be an ideal nanomaterial for membrane technology due to their great compatibility with polymer matrices and also decrease the number of interface defects and improve the stability of the

Table 1 COF-based composite membranes for water purification and desalination applications[a]

Type of membrane	Fabrication method	Membrane structure/thickness	Feed solution	Permeance (L m^{-2} h^{-1} bar^{-1})	Rejection (%)	Ref.
TpPa-1	CVD	1 μm	AOR	50.83	90.98	156
			RhB		91.99	
			CV		96.18	
			CR		96.37	
			MB		98.78	
			AnB		98.78	
TFB-PDA (COFLZU1)	Pressure-modulated	—	Na_2SO_4	44.2	63.6	157
			NaCl		20	
Carboxylated COF	Blending	80–130 μm	BSA	940	81.9	158
			γ-Globulin		99.4	
TpEBr	Blending	150–200 nm	BSA	380.1	92.6	155
TpPa-2	Blending	91.5–95.8 μm	HA	200.1	92	159
TpOMe-Azo	Self-standing	320 μm	MB	170	99.9	160
			RB		99.9	
			RhB		99.4	
			CR		99.9	
$TpPa(OH)_2$	Self-standing	25–120 μm	NaCl		62.9	161
			KCl		51.4	
			$CaCl_2$		60.7	
			$MgSO_4$		62.8	
TFP-PDA (TpPa-1)	Solid-vapor IP	120 nm	AB	411	99.1	162
			PPH-IX		98.9	
			CR		98.9	
			MB		98.1	
			OG		85.4	
TpBD	Solid state mixing	405 μm	VB12	91.6	99	79
			RB		99	
			CR		96	
			MB		94	
			TC		95	
			CM		83	
TpTD	Solid state mixing	440 μm	VB12	117.6	96	
			RB		84	
			CR		81	
			MB		83	
			TC		86	
			CM		78	
COF-LZU1	Solvothermal	400 nm	CBT	75.60	98.2	151
			MB		99.2	
			CR		98.6	
			AF		91.4	
			RB		99.1	
TpPa-1	Solvothermal	—	BSA	1173	92.3	163
			CR	14	99.4	
			AF		97.2	
			RB19		98.7	
			CBT		99.1	
			AO7		80.2	
IISERP COOH-COF1	Solvothermal	3.2 μm	Na_2SO_4	0.56	96.3	164
			$MgSO_4$		97.2	
			$FeCl_2$		99.6	
			$MgCl_2$		90.6	
			NaCl		82.9	
TpPa-1-BCP	Solvothermal	450 nm	MB	51	98	165
			CR		98	
			CBT		98	
			AF		87	
COF-300	Solvothermal	5.5 μm	RB	85	99.5	166
			MB		99.0	
			CR		98.7	
			CBT		97.7	
			AB25		91.7	
			MO		78.3	

Table 1 (*Contd.*)

Type of membrane	Fabrication method	Membrane structure/thickness	Feed solution	Permeance (L m^{-2} h^{-1} bar^{-1})	Rejection (%)	Ref.
ACOF-1-BCP	Solvothermal	662 nm	Na_2SO_4	0.57	95.7	167
			$MgSO_4$		90.2	
			$MgCl_2$		69.6	
			NaCl		43.0	
TFB-PDA (COF-LZU1)	*In situ* growth	—	RhB	200	89.7	168
			CR		99	
			DR80		99	
TpPa-1-pDA	*In situ* linker exchange		Na_2SO_4	50–60	99.5	123
			$MgSO_4$		91.3	
			$MgCl_2$		70.3	
			NaCl		49.2	
COF	*In situ* growth	—	Na_2SO_4	—	97	105
TAPB-PDA	IP	10–50 nm	R-WT	0.012 m per day	90	60
TAPB-PDA	IP	2.5 nm to 200 μm	RWT	0.2–0.8 m per day	91	58
TpPa-1	IP	500 nm	CR	50	99.5	62
			MB		94.4	
			CB		96.3	
			AF		52.6	
			AO7		14.7	
TbTG COFM	IP		NaCl		93.3	110
			$MgCl_2$		99.5	
			Na_2SO_4		98.7	
			$MgSO_4$		99.1	
Imine-COF	IP		MLB	67.37	98.7	169
TpEBr	LbL stacking	189 μm	MO	546	99.6	152
			FSs		99.2	
			PP		98.1	
			RhB		91.2	
			MB		87.2	
			DMPD		84.9	
			CA		74.4	
			NR		22.3	
			NA		15.7	
TAPB-PDA-H	IP	20 nm	R-WT	0.009 m per day	71.0	150
TAPB-PDA-Me			R-WT	0.006 m per day	77.0	
TAPB-PDA-Et			R-WT	0.0021 m per day	86.2	
TFB-PDA (COFLZU1)-GO	LbL stacking	2.7 μm	MB	59	99	170
			CR		99.82	
COF-9	LbL stacking	800 nm	OCT_4	2260	100	116
			$Dodecyl_4N^+$		100	
TpPa-1	LbL synthesis		CR	265	99.8	76
			MB		80	
			AF		50	
TpBD		6 μm	CR	339	98.6	
			MB		75	
			AF		25	
CTF-1-GO	LbL stacking	32 nm	CBT	226.3	98.9	68
			MB		94.8	
			CR		93.1	
			AB		91.8	
TpPa-1-GO	LB		CV	166.8	98.24	171
			MB		97.05	
			ACBK		68.57	
TpPa-1	IP	65 nm	OG	41.85	93.91	172
			MB		99	
			CR		99	
			AB		99	
TFP-DABA	IP	42 nm	CR	134.6	99.1	173
			CBT		99.2	
			MB		93.1	
			AB		94.0	

Table 1 (*Contd.*)

Type of membrane	Fabrication method	Membrane structure/thickness	Feed solution	Permeance (L m^{-2} h^{-1} bar^{-1})	Rejection (%)	Ref.
TpPa-1	IP	6.5 μm	MO	60	82.8	174
			CBT		84.7%	
			AF		90.4	
			RB19		92.7	
			CR		98.7	
			MB		96.5	
			EB		98.5	
T_pTG_{Cl}-CNFs	LbL stacking		CR	70–80	99.6	48
			AB		98.3	
			MB		90.3	
			OG		90.3	
			Na_2SO_4	42.8	96.8	
			$MgSO_4$		95	
			$MgCl_2$		50	
			$CaCl_2$		40	
			NaCl		25	
COF-1-GO		100–250 nm	CR	31.09	99.62	175
			MB		99.04	
			RB5		99.49	
			DR		98.95	
			CBT		100	
COF-LZU1	LbL synthesis	300 nm	AOR	46.51	92.41	192
			CBT		94.24	
			AF		96.50	
			AnB		99.43	
			MB		98.34	
TAPT-PAD	LbL	22 μm	AF	282.2	67.3	193
			CR		99.8	
			MB		85.6	
			AB		90.2	
		31 μm	AF	73.0	86.1	
			CR		99.9	
			MB		94.7	
			AB		96.8	
TpBD	LbL stacking	250 nm	EB	88.9	99.2	154
			MB		95	
			EY		80	
			AF		80	
			MO		30	
COFLZU-prGO		200 nm	MB	194.0	98	176
			AO7		98	
			RhB		98	
TpBpy	IP	2.1 μm	BB	211.5	94	61
			CR		80	
			AF		97	
			RhB		98	
			TB		97	
TpAzo	IP	5.3 μm	BB	45.9	90	
			CR		79	
			AF		99	
			RhB		99	
			TB		96	
TpPa-1-PA	IP	120 nm	MB	17.14	99	177
			CR		99	
			CBT		99	
			Na_2SO_4		93	
			$MgSO_4$		65	
			$MgCL_2$		22	
			NaCl		25	
TpBD	IP	100 nm	AOII	33.6	88.8	65
			AF		92.5	
			MB		99.1	
			CR		99.6	

Table 1 (*Contd.*)

Type of membrane	Fabrication method	Membrane structure/thickness	Feed solution	Permeance (L m^{-2} h^{-1} bar^{-1})	Rejection (%)	Ref.
TpBDMe	IP		AOII	62.2	80.9	
			AF		81.9	
			MB		98.7	
			CR		99.1	
			CBT		99.9	
TpAD-50	LbL stacking		DR80	593	98.5	178
			DR23		98.3	
			CR		82	
			RhB		98	
			MV		88.3	
CTF-1	LbL stacking	77 nm	CBT	64.9	97.4	179
			AF		92.4	
			CR		97.9	
			MO		56.9	
TpPa-SO_3Na	IP	2.2–2.4 μm	MeB	209	99.8	180
			EBr		99.5	
			NR		24.4	
			NA		16.7	
			MO		87.6	
			FSs		84.1	
TFB-PDA (COF-LZU1)	IP	200 nm	DB38	80	99.5	64
			CBT		99.5	
			CR		83	
			AF		83	
			MeB		63	
			RhB		40	
SNW-1-PA	IP	300 nm	Na_2SO_4	19.25	83.5	181
			$MgSO_4$		70	
			NaCl		15	
TPA-Tru$(NH_2)_3$	IP	4.7 nm	$MgSO_4$	0.74	71.34	72
			NaCl		62.27	
TpPa-1-Pda-PA	IP	11 nm	Na_2SO_4	20.71	93.4	55
			$MgSO_4$		90	
			$MgCl_2$		20	
			NaCl		20	
TpPa-1-PA	IP	82 nm	Na_2SO_4	53.55	94.3	182
			$MgSO_4$		80.7	
			$MgCl_2$		37.6	
			$CaCl_2$		33.8	
			NaCl		27.3	
$TpTG_{Cl}$-PA	IP	670 nm	Na_2SO_4	31.1	95	183
			$MgSO_4$		90	
			$MgCl_2$		52	
			NaCl		12	
CTF-1 PA	IP	168 nm	Na_2SO_4	45.6	93.5	184
			$MgSO_4$		92	
			$MgCl_2$		45	
			NaCl		17.5	
TpPa-1-PA	IP	150 nm	NaCl	1.68	99.2	185
NENP-1-PSA	IP	61.3 nm	$CaCl_2$	15.1	94.9	63
			$ZnCl_2$		93.8	
			$MgCl_2$		93.3	
			Pb $(NO_3)_2$		92.2	
			$MgSO_4$		90.2	
			NaCl		58.2	
			Na_2SO_4		54.3	
TpHz	IP	500 nm	Na_2SO_4	4.05	58.3	186
			$MgSO_4$		45.3	
			$CaCl_2$		35.2	
			$MgCl_2$		31.0	
			NaCl		6.7	
TpPa-2-PA	IP	130 nm	NaCl	2.2	92.5	187

Table 1 (*Contd.*)

Type of membrane	Fabrication method	Membrane structure/thickness	Feed solution	Permeance (L m^{-2} h^{-1} bar^{-1})	Rejection (%)	Ref.
TMC-PPD(PDA)-PA	IP	100 nm	NaCl	2.5	92.5	188
TpBD-NH_2-PA	IP	23.2 nm	Na_2SO_4	6.0	98.1	189
			$MgSO_4$		92.5	
			$MgCl_2$		35	
			NaCl		20	
TpPa-1-TMC	IP	74 nm	Na_2SO_4	0.81	96.6	190
			$MgSO_4$		96.0	
			$MgCl_2$		93.3	
CTF-1-PA	IP	176 nm	Na_2SO_4	23.8	95.3	53
			$MgSO_4$		93.6	
			$MgCl_2$		75	
			NaCl		70	
TFP-DHF	IP	61.2 nm	RG	60	99	59
			VB12		98	
			ReB		96	
			CR		80	
SNW-1-PA	IP	80 nm	RhB	7.98	99.4	191

[a] AF, acid fuchsin; TB, thymolphthalein blue; CR, Congo red; BB, brilliant blue; AB, Alcian blue; MB, methyl blue; and OG, orange GII.

membrane. To date, multiple COFs with borate, hydrazine, imine, and triazine structures have been reported. COFs can be fabricated into pristine and composite membranes as well as being used as fillers in mixed matrix membranes, as shown in Table 1. COF laminates are mostly prepared by bottom-up approaches including solution-based synthesis or chemical vapor deposition. In addition, top-down approaches, such as liquid phase exfoliation, ball milling, mechanical cleavage and intercalation and exfoliation are also commonly used. Besides these methods, interfacial polymerization, solid-state mixing *in situ* growth approach, assembly of COF nanosheets, unidirectional diffusion synthesis, vacuum filtration, spin coating, Langmuir–Blodget assembly, layer-by-layer synthesis, direct evaporation or drop casting, *etc.* are also widely used for preparation of COF-based lamellar membranes, as shown in Table 1. In this section, we summarize the current fabrication techniques used for preparation of COF-based lamellar membranes, and discuss their main issues and engineering challenges.

2.1. Interfacial polymerization method

Interfacial polymerization (IP) is a polycondensation reaction in which a polymer is synthesized at the interface of two liquids, each of which contains one or more reactive monomers. IP is widely used to prepare large-area and defect-free membranes.[51–53] Recently, COF thin film membranes have been produced in large quantities using the IP approach at constrained interfaces.[48,54–57] Several works have been published on the IP method for fabrication of self-supported COF films at the liquid–liquid interface, which could then be transferred onto a porous substrate using a variety of techniques to prepare composite membranes.[58–60] The fabrication of COF membranes by the IP method without the transfer procedure was suggested in order to fabricate COF composite membranes with exceptional mechanical properties. By using water–organic interfacial polymerization, Banerjee and colleagues demonstrated a ground-breaking experiment for fabricating large-scale thin COF membranes in ambient conditions.[61] Dichloromethane was used to dissolve the aldehyde organic cross-linker, while water was used to dissolve the amine monomers. Amines were first salt-mediated by tosylic acid (TsOH) to improve their solubility as monomers. TsOH can work as a catalyst for the organic Schiff base reaction in addition to making amine more soluble. Wang *et al.* fabricated a COF membrane on a PSF ultrafiltration support using the *in situ* interfacial synthesis method.[62] Due to its micron-thickness, the obtained COF/PSF membrane has a comparatively low water permeability, but it is capable of achieving a high level of dye separation. Li *et al.* synthesized an NENP-1@PSA@PES membrane by the IP method.[63] The authors combined triazine-structured COF nanosheets (NENP-1) with polysulfamide layers. The NENP-1 achieved the synergy of improved hydrophilicity and positive charge ability with suitable pore sizes and was responsible for good water permeance and high rejection of ions. Meanwhile, NENP-1 was covalently connected to the PSA matrix and enhanced the stability of the membrane. Due to this chemical linkage, the acidity resistance of this membrane was exceptionally high. Lang *et al.* fabricated an LZU1@COF membrane on a polyether sulfone (PES) support using the *in situ* IP method.[64] This membrane showed good water permeance and excellent dye rejection. Wang and coworkers reported a COF membrane with controlled pore structure by an *in situ* IP method.[65] Liu and coauthors used the IP method to prepare an ACOF-1 nanocomposite membrane with azine linkage on the hydrolyzed polyacrylonitrile support (Fig. 3a and b).[54] This membrane can be used for separation of ions, toxic molecules and mixtures due to its ideal aperture in nm

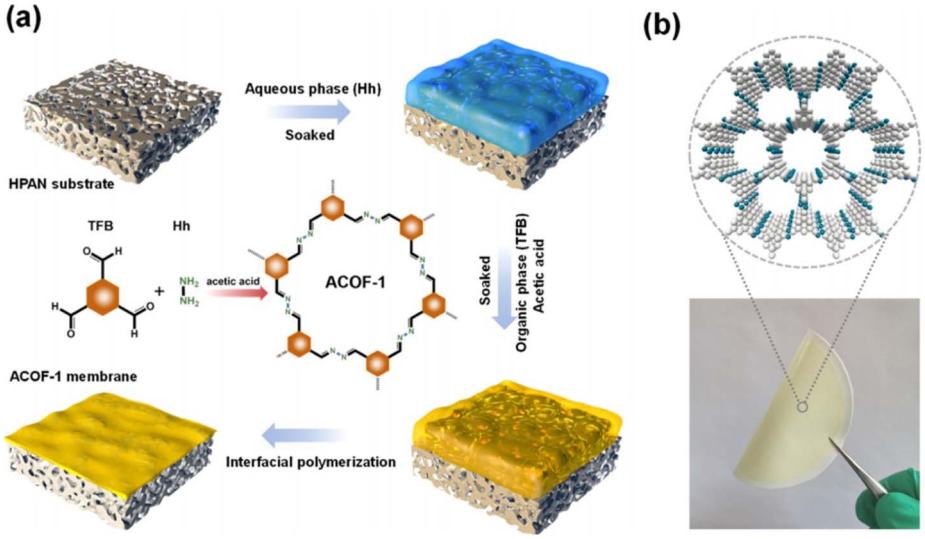

Fig. 3 (a and b) Schematic illustration of the IP method used for preparation of the ACOF-1@HPAN membrane and its digital photograph, respectively. Data obtained with permission.[54] Copyrights 2021, American Chemical Society.

and good chemical stability. The polyacrylonitrile (PAN) substrate was immersed in hydrazine hydrate aqueous solution and 1,3,5-triformylbenzene organic phase solution. The defect-free and continuous membrane was obtained as a final product. During this process, the original micro-pores of the support were filled by the ACOF-1 layer. Even though a lot of work has been reported on the fabrication of COF membranes using IP techniques, it is still not enough to meet the demands that are being placed on researchers today.

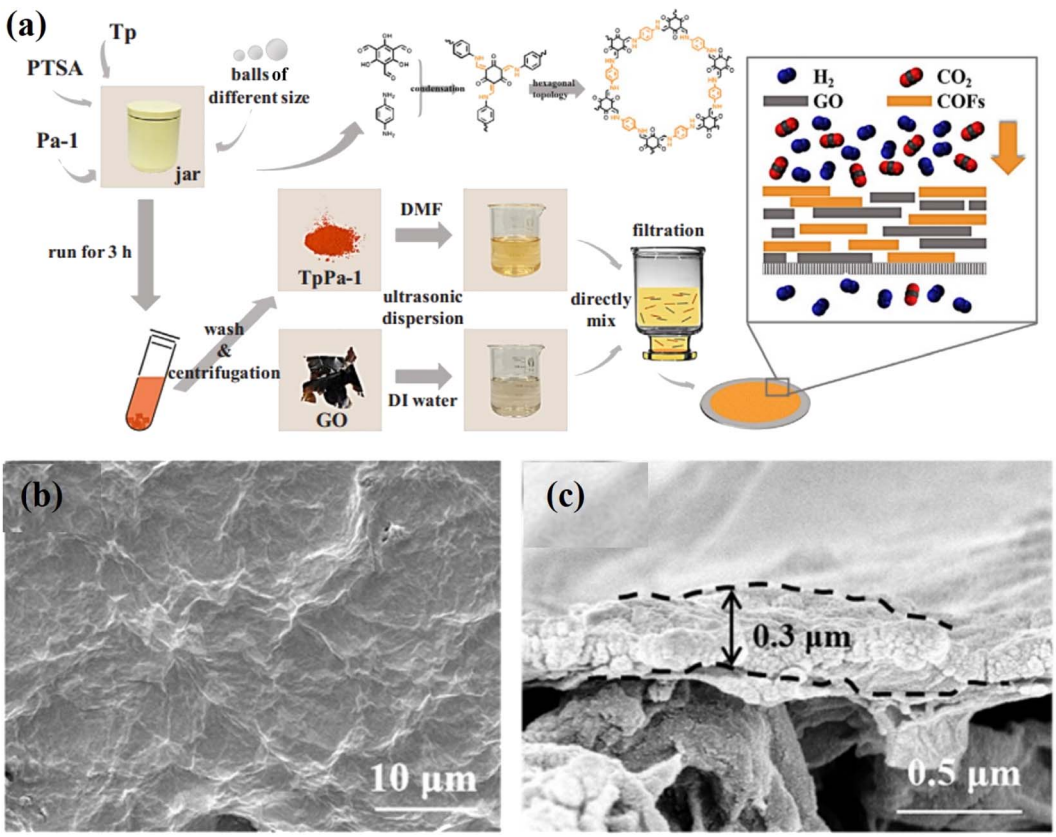

Fig. 4 (a) Schematic diagram of the fabrication of the TpPa-1/GO composite membrane using the VF method and a sketch of the gas separation test. (b and c) Surface and cross-sectional SEM images of the TpPa-1/GO composite membrane. Data obtained with permission.[70] Copyright 2019, Elsevier.

2.2. Vacuum filtration (VF) method

VF is the most simple and popular method used for synthesis of 2D COF laminates.[48,66–69] The primary advantage of this process is that it does not alter the physiochemical properties of the 2D nanosheets because it does not involve covalent bonding. Its thickness is mostly influenced by the amount and type of suspension that is filtered through the VF assembly. COF membranes prepared by the VF method are typically deposited on supporting membranes, such as anodic aluminium oxide, polymers, *etc.* Tang *et al.* used the VF method to deposit TpPa/GO layers on a nylon substrate, as illustrated in Fig. 4a–c.[70] Yang *et al.* used 1D cellulose nanofibers to modify 2D COF nanosheets and fabricated several membranes with controlled nanochannels (0.45 to 1 nm) *via* the VF method.[48] Due to the dense packing of 2D nanosheets, this technique is normally time-consuming. Specifically, an asymmetric membrane structure with an uneven upper surface and a smooth lower surface could be obtained. During the initial phase of filtration, the 2D nanosheets stack uniformly, but as the deposition thickness increases, the mode of water loss shifts from filtration to evaporation. It has been reported that, unlike vacuum-assisted filtration, pressure-assisted filtration produces a denser and more uniform laminated structure under two-way pressure. However, the filtration system limits its depositional area. In the laboratory, VF is the most prevalent method for fabricating ultrathin and uniform laminated membranes.

2.3. Langmuir–Blodgett method

The Langmuir–Blodgett (LB) approach (Fig. 5) has been frequently used to prepare 2D laminates in recent years.[71] The LB method is a possible technique for producing large scale membranes with adjustable dimensions that are simple to transfer to various support surfaces. This method can be ideal to control the thickness and layers of 2D sheets. The trough needs to be well cleaned, rinsed with chloroform, and then filled with de-ionized (DI) water in order to fabricate a COF membrane using this approach. Using a glass syringe and a tensiometer to measure the surface pressure, the COF dispersion was applied to the water's surface gently and at a regulated rate. After compression, the COF membrane with a light brown color was produced. The substrate was lowered into the trough vertically and slowly pulled up to transfer it. By using the LB approach, Shinde *et al.* synthesized crystalline COF films at the liquid–air interface and subsequently transferred them onto various supports to prepare multilayered COF membranes.[59] No doubt this method is successful up to a certain extent, but it is more time-consuming and complex. Additionally, there are still other issues related with the mechanical properties of the resulting COF composite films as well as the bonding force between the COF films and porous substrates. Gadwal and coworkers[72] prepared a 2D COF membrane with pore size of ~1.5 nm using the LB method. The as-prepared membrane showed good ionic sieving properties, such as NaCl (64%) and $MgCl_2$ (71%). Shevate *et al.*[58] fabricated a large-area ketoenamine-linked COF membrane with thickness of 24 nm by the LB approach. Direct integration of variable-length monomers is able to adjust the single-digit nanopore size (1.4–2.0 nm) at the angstrom level, as illustrated in Fig. 3.

2.4. Layer-by-layer assembly method

The layer-by-layer (LbL) method, also referred to as the step-by-step method, is a potential bottom-up technique for synthesizing ultrathin COF laminates. It provides a methodical way to prepare COF laminates with precise control over the thickness at all scales, from the monolayer to the multilayer.[73] The LbL assembly process typically entails the cyclic, easy alternate deposition of species with a variety of chemical

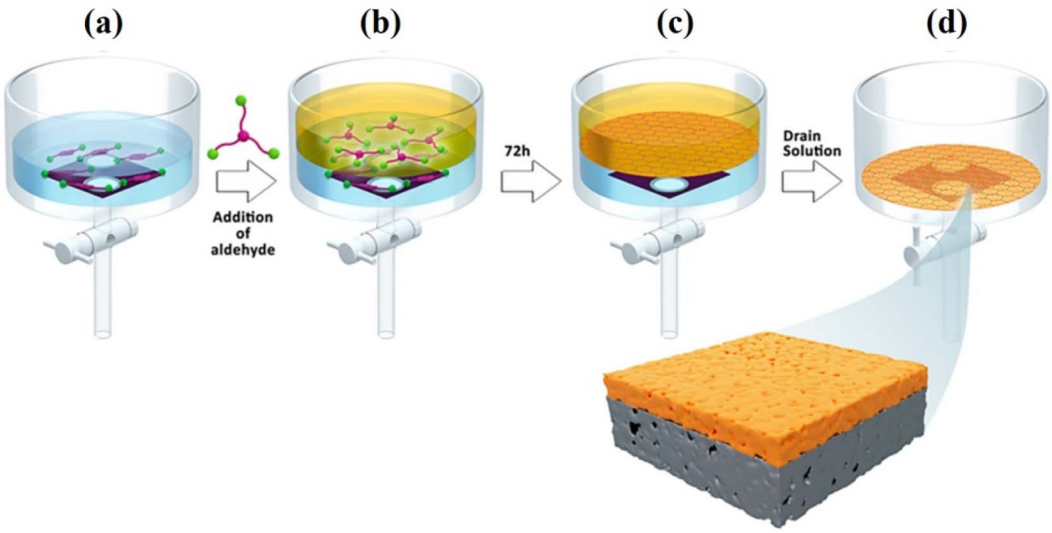

Fig. 5 LB fabrication method: (a) the bottom of the trough was lined with a porous support, followed by the addition of the TsOH catalyst and aqueous diamine solution on top. (b) The formation of a liquid–liquid interface with the addition of an aldehyde solution on top of an aqueous solution. (c) Self-assembled formation of the COF membrane obtained after 72 h at ambient temperature. (d) The discarding of solvent from the bottom of the trough and formation of a supported COF membrane. Data obtained with permission.[58] Copyright 2018, Elsevier.

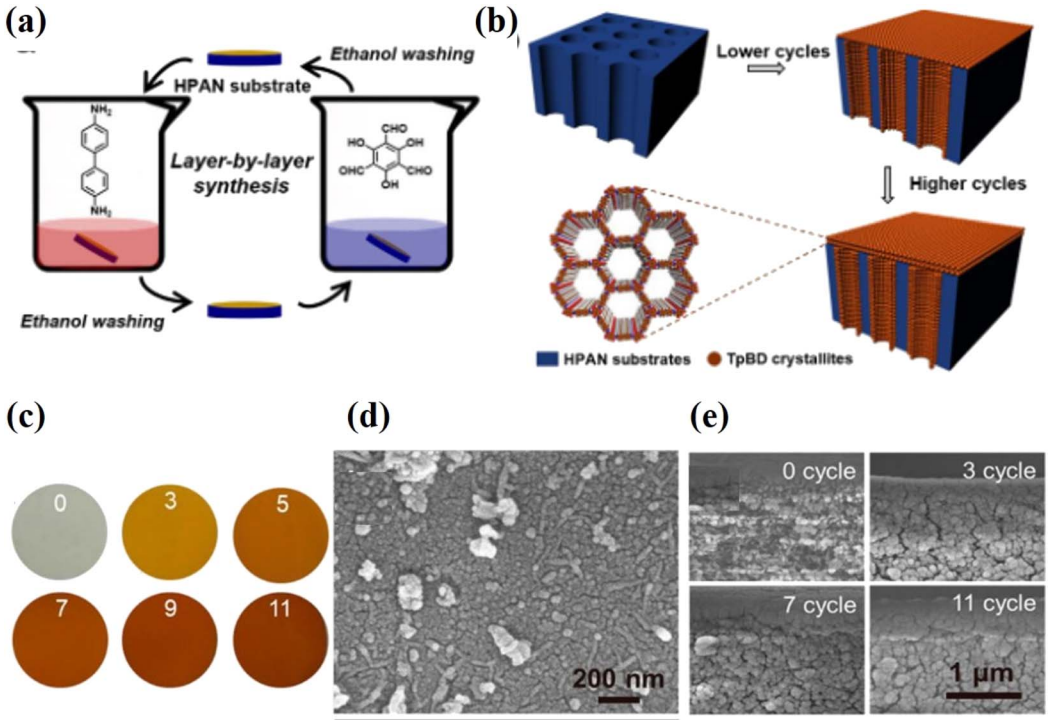

Fig. 6 Diagrammatic representation of the LbL-synthesised TpBD-HPAN membranes. (a) The steps involved in the LbL synthesis process. (b) A schematic representation of TpBD crystallites that have grown on an HPAN substrate. (c) Photographs of the TpBD-HPAN membranes after they had been subjected to a variety of LbL cycles. (d) The structure of the TpBD11-HPAN membrane's outermost layer. (e) Membrane cross-sectional morphologies produced by 0, 3, 7, and 11 LbL cycles. All four images have the same magnification. Data obtained with permission.[76] Copyright 2018, American Chemical Society.

interactions and surface functionalization to construct and regulate the composite film.[74] Li *et al.* used a solution of COF-1 nanosheets to coat a macroporous Al_2O_3 substrate with a thin SiO_2–ZrO_2 intermediate layer to create a highly permeable membrane that was pinhole and crack free.[45] Ying *et al.* reported COF membranes with a thickness of only 300 nm by re-

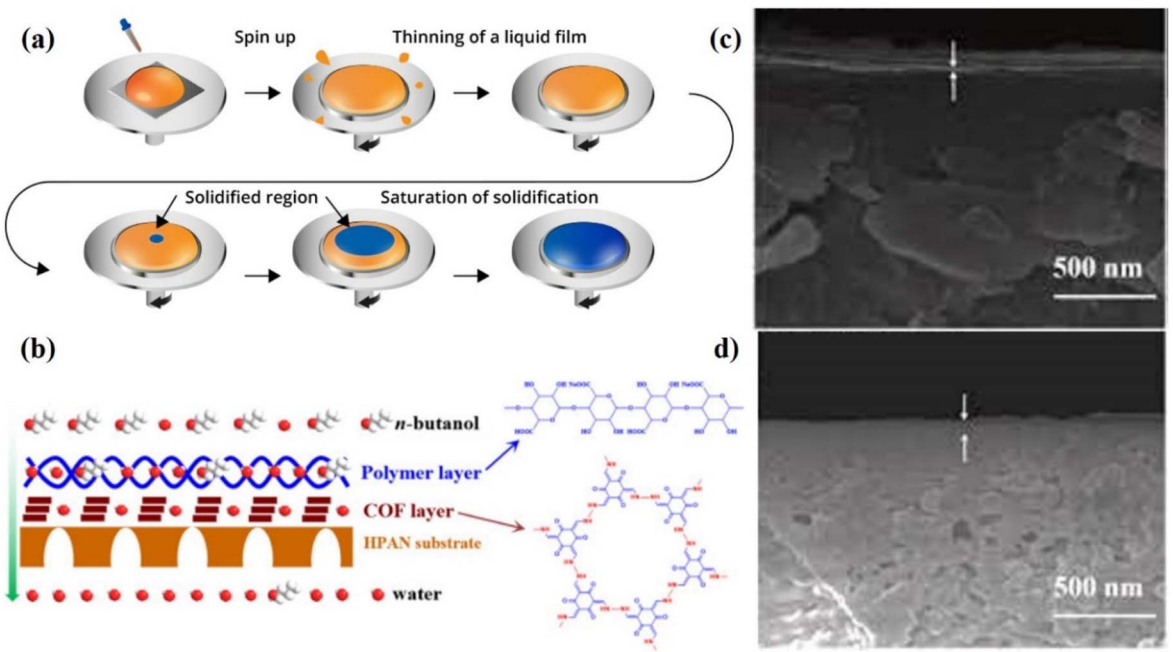

Fig. 7 (a) Spin coating method. (b) A diagrammatic representation of the suggested membrane structure for the separation process resulting from the synergy between the calcium alginate layer and the COF layer. (c and d) Cross-sectional SEM images of the COF/HPAN and Alg-Ca/COF/HPAN membranes, respectively. Data obtained with permission.[77] Copyright 2019, Elsevier.

stacking a mixture of GO nanosheets and covalent triazine-based framework-1 in water.[67] Zhao *et al.* demonstrated a COF membrane by putting together two types of ionic covalent organic nanosheets (iCONs) with different pore sizes and opposite charges.[75] Because the iCONs are packed in an uneven pattern and have strong electrostatic interactions, the resulting membranes have smaller holes, an optimized stacking pattern, and a compact, dense structure without giving up control over the thickness. Shi *et al.* reported imine-linked COF membranes (TpBD-HPAN) on a porous polymeric support in ethanol at room temperature using the LbL method,[76] as shown in Fig. 6a and b. This approach takes advantage of the fact that each COF monomer is available in different ways to make the reaction self-limiting. As a result, COFs grow in a straight line along the pore wall of the substrate. The grown COFs with thicknesses that can be changed by LbL cycles make the pores smaller, and the 2 nm channels in COFs let more water through (Fig. 6c–e). The as-prepared membranes have much better selectivity (>99% rejection of dyes) and water permeances 3–20 times higher than those of other membranes. This work might show a new, general way to make COF membranes based on imines that can be used to separate molecules.

2.5. Spin coating method

Spin coating is a process that utilizes centrifugal force to apply a uniform film onto a solid surface and necessitates a liquid–vapor interface (Fig. 7a). This coating needs a special spin coating machine. In this method, a COF mixture with a known concentration is put in the middle of the substrate and spun at high speed (rpm) with the help of a spin coating machine. The solvent is then evaporated to get a uniform film or membrane. During spin coating, centrifugal force is a key factor in making sure that the dispersion is spread out evenly on the material. Usually, the thickness of a membrane depends on the concentration of the dispersion, the volume, and the speed of the machine. The major benefits of this process are that it saves time and makes it possible to get a very fine, even coating. But the size of the base can cause problems. As the size of the base gets bigger, it gets harder to spin at a high speed, which makes it harder to spread the material

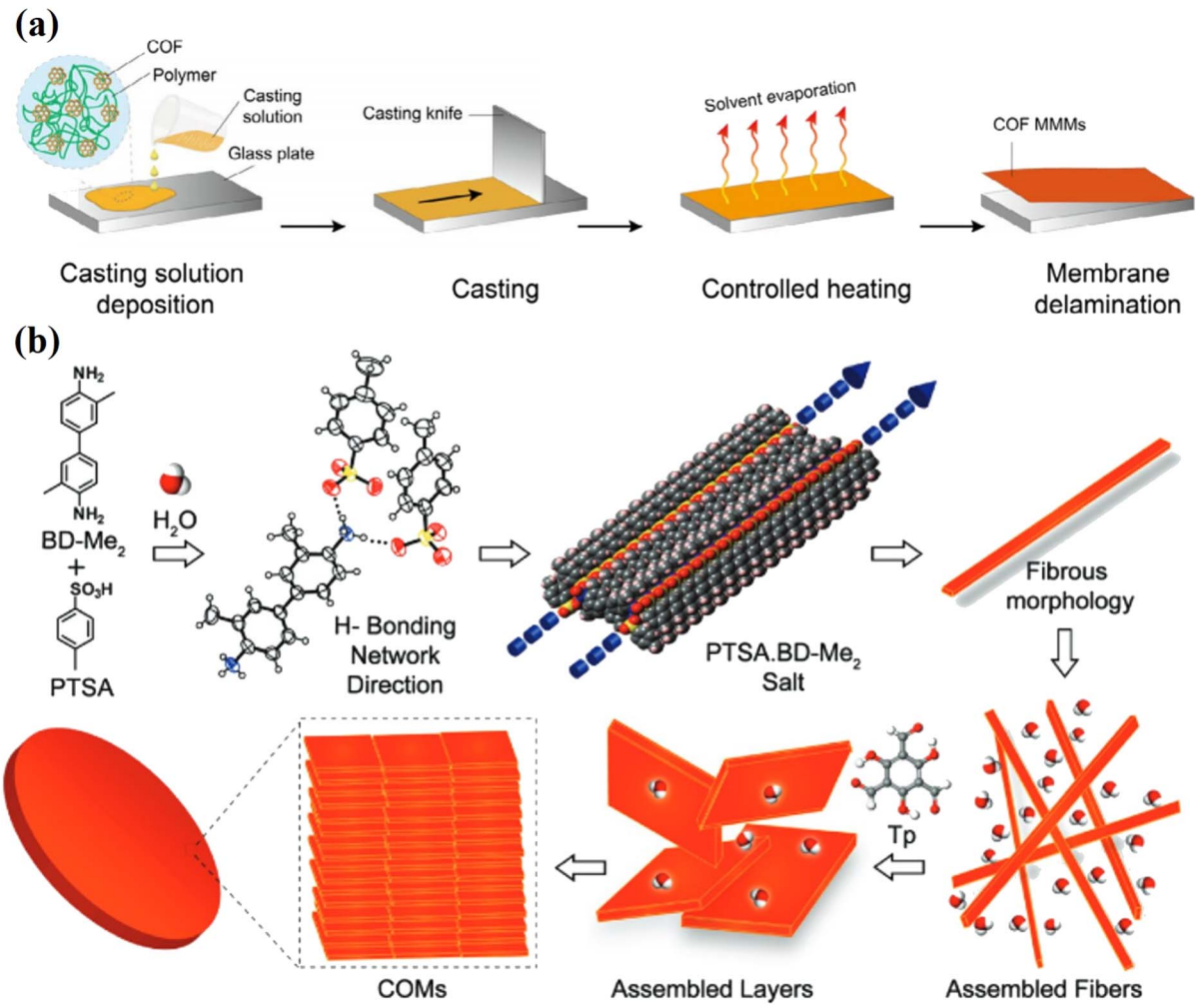

Fig. 8 (a) Schematic diagram of the casting solution method for fabrication of COF-based membranes. Data obtained with permission.[81] Copyright 2021, Wiley-VCH. (b) Proposed preparation mechanism and morphological evaluation of COF-membranes (M-TpBD-Me_2). Data obtained with permission.[79] Copyright 2017, Wiley-VCH.

evenly. The other main problem is that it does not work well with water solvent, while all other solvents are expensive compared to water. Therefore, it is not a cost-effective method compared to other reported methods. Liu *et al.* deposited a 2D COF layer on a porous support with the help of the spin coating technique,[77] as shown in Fig. 7b. As shown in Fig. 7c and d, the SEM studies clearly showed that the membranes are made up of a porous base and a tightly coated thin active layer with no interfacial defects. Due to the structure of the COF, this membrane was able to do two things at once: on the one hand, it made it easier for water molecules to stick to it, and on the other, it acted as a molecular screen during the alcohol dehydration process.

2.6. Casting solution method

COF-based laminates are also prepared using the casting solution method, as shown in Fig. 8a.[78] Banerjee *et al.* prepared highly porous and free-standing COF membranes (M-TpBD and M-TpTD) using the casting solution method (Fig. 8b).[79] This method is cheap and easy to scale up because it involves baking the sample dough that had been pressed with a knife onto a glass plate. Using a similar method, Banerjee *et al.* made three different COF membranes with a thickness of more than 100 nm by slowly baking symmetrical organic linkers for three to four days at a reasonable temperature with amino TsOH and water.[80] In this work, the co-reagent TsOH : H_2O worked as a proton transporter and also made the membranes more porous and crystalline, which increases proton conductivity.

3. Water purification and desalination applications

Population growth, urbanization, economic development, and climate change will all cause a 55% increase in the world's water consumption during the next 30 years. Poor sanitation in the developing world and reuse of wastewater in developed countries have led to a growing number of pollutants such as salts, heavy metal ions, bio-organism, organic dyes, antibiotics, oil, *etc*. in the water, that damage water supplies and public health.[82–89] The separation and degradation of these pollutants are not an easy task due to their complex nature and very small size. In this regard, membrane technology offers a cost-effective approach to remove these pollutants from water. Nanofiltration and reverse osmosis-based membrane technology are key separation processes used for treatment of sea water, brackish water, and industrial wastewater, which can effectively remove pathogens and other inorganic and organic pollutants. The efficiency of a membrane usually depends on its material. In this regard, several materials, such as polymers, ceramic, silica, porous carbon, and zeolite, have been tested for purification of sea water and industrial effluent. These materials showed an outstanding separation for targeted molecules or ions, and most of them are commercially used for purification applications. However, still they are facing several issues related to their low stability, high cost and fouling problems. Therefore, it will be a big milestone for scientists to produce cost-effective membranes in future with extraordinary separation properties. Recently, graphene,[90–93] MXene,[94–96] TMDCs,[97,98] COFs,[99–101] MOFs,[26,102,103] and other 2D material-based membranes have been successfully utilized for water purification and desalination. Among them, COF-based membranes (Table 1) have been proven to be one of the best platforms for producing size-selective ionic and molecular separation membranes because of their adjustable pore size, ultrathin thickness, high porosity, exceptional mechanical strength, well-organized pore structures, and chemical inertness.[104–116] In this section, the ionic and molecular separation properties of COF laminates are discussed in detail.

Theoretical studies suggested that COF membranes have great potential to separate salt and toxic dyes. COF membranes with large pore size (1.58 nm) do not reject ions, but show higher water permeance than commercial membranes.[111] On the other hand, COF membranes with small pore size (0.8 nm) show little more rejection (~45%) for NaCl salt.[117] This rejection is attributed to their controlled nanochannel size and hydrogen bonding interaction between polar functional groups and hydrated ions. Zhang *et al.* theoretically studied the water desalination properties of several membranes based on 2D COF (TpPa-1).[118] These results demonstrated the high water permeability of the membranes ranging from 1216 to 3375 kg m^{-2} h^{-1} bar^{-1}, which is several times higher than that of commercial RO membranes. This exceptionally high water permeance of the membranes is possibly due to their mono-atomic thickness. Further, it is more interesting that these membranes showed salt rejection >98%. This theoretical study clearly demonstrated that rejection of salt is not only dependent on the pore size of membranes. Because membranes with low *d*-spacings such as TpPa-AMCOOH (0.53 nm) and pPA-AM3 (0.51 nm) must show high rejection for salts, they showed the lowest slat rejection compared to other membranes with large pore size. But high rejection of salts is attributed to the functional group, smallest *d*-spacing and hydrophobic nature. On the other hand, multilayer COF membranes showed high rejection, however it is very difficult to achieve the same permeance in multilayered COF films, in which the stacking layers and numbers of COF monolayers play significant roles.

Experimentally, several membranes based on COF 2D materials have been widely explored for ionic separation. Recently, self-supporting COF membranes have also been used in the nanofiltration (NF) process to capture divalent ions and other ions. Sheng *et al.* fabricated a 20 nm-thick $TpBDMe_2$-based laminate with 1.4 nm pore size and plenty of hydrogen bonding sites (Fig. 9a).[119] This membrane showed water permeance between 0.1 and 0.2 mol m^{-2} h^{-1} for monovalent cations and low permeability for multivalent cations. Although this membrane has a large interlayer spacing of 1.4 nm, the membrane still showed very low permeance. On the other hand, significant rejection for monovalent ions was achieved over divalent ions, such as K^+/Mg^{2+} (765), Na^+/Mg^{2+} (680), and Li^+/Mg^{2+} (217). Both experimental results and theoretical predictions suggested that hydrogen bonding interactions between functionalities and hydrated ions played an important role in ion selectivity. Shen *et al.* obtained 98.3% rejection for Na_2SO_4 and water permeance of 13.1 L m^{-2} h^{-1} bar^{-1} using a TpPa-

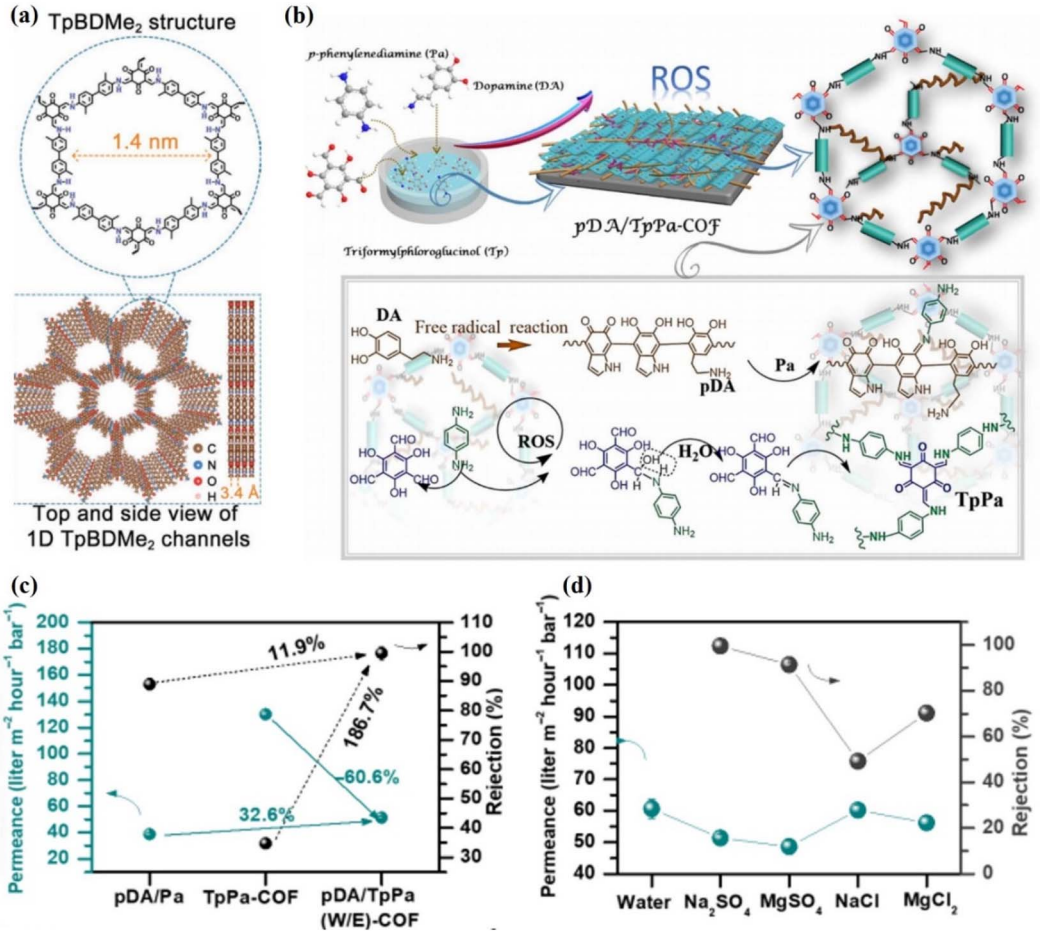

Fig. 9 (a) $TpBDMe_2$ membrane's structure from the top and side, showing the 1.4 nm hydrogen bonding sites on the channel wall and 1D nanochannels. Data obtained with permission.[119] Copyright 2021, Wiley-VCH. (b) The step-by-step procedure of *in situ* molecular soldering engineering used to synthesize a pDA/TpPA-COF membrane. (c) The permeability and rejection of the pDA/TpPa(W/E)-COF membrane, the pDA/Pa membrane, and the TpPa-COF membrane were used to separate Na_2SO_4. (d) The performance of the pDA/TpPa(W/E)-COF membrane in terms of salt separation. Data obtained with permission.[123] Copyright 2021, Science.

SO_3H@TpPa-SO_3H@MPAN membrane.[120] The commercial membrane usually required 120 to 400 L m^{-2} h^{-1} bar^{-1} water permeance. Therefore, these membranes cannot be scaled up due to their low permeance. Khan *et al.* prepared a polyamide@covalent triazine framework nanosheets@thin-film composite membrane.[53] The authors introduced additional water nanochannels in the form of pores in interfacial cavities by incorporating covalent triazine framework nanosheets into the polyamide matrix. Due to these additional nanochannels, the membrane exhibited high water permeance up to 23.8 L m^{-2} h^{-1} bar^{-1} along with >95% rejection for Na_2SO_4. Wu *et al.* achieved 93.4% rejection of Na_2SO_4 through a PA@PDA-COF@PAN membrane and a remarkable water permeation of 207.07 L m^{-2} h^{-1} MPa^{-1}.[55] Jiang *et al.*[121] rejected NaCl up to 93% using a COF membrane and obtained a maximum water permeance of 3.7 L m^{-2} h^{-1} bar^{-1}. Zheng *et al.* prepared TpPa-SO_3H/PAN COF membranes *via* a counter-diffusion method and obtained 97.4% rejection for Na_2SO_4 salt.[122] Li *et al.* fabricated a TbTG/COF membrane with a low interlayer spacing of 0.4 nm.[110] Due to the low interlayer spacing, this membrane exhibited high rejection of NaCl (93.3%), $MgCl_2$ (99.5%), Na_2SO_4 (98.7%), and $MgSO_4$ (99.5%). It is more interesting that the membrane maintained high salt rejection for 10 000 ppm concentration of salts and high pH values of 9.4. Zhang *et al.* fabricated defect-free TpPa-COF and pDA/TpPA(W/E)-COF membranes with superior antifouling and water desalination properties (Fig. 9b).[123] Due to their layered structures and persistent porosity, the TpPa-COF and pDA/TpPa(W/E)-COF membranes exhibited a high capacity for water absorption. The 1253 nm-thick pDA/TpPa(W/E)-COF membrane showed good rejection of 99.5% for Na_2SO_4 along with water permeance of 51.3 L m^{-2} h^{-1} bar^{-1} compared to the pDA/Pa membrane (~38.7 L m^{-2} h^{-1} bar^{-1}), as shown in Fig. 9c. Further, the performance of the membrane was evaluated using monovalent and divalent salts at 5 bar with 1000 ppm feed solution. The membrane showed 99.5%, 91.3, 70.3% and 49.2% rejection for Na_2SO_4, $MgSO_4$, $MgCl_2$, and NaCl, respectively (Fig. 9d). The low rejection of $MgCl_2$ and NaCl salts is due to the small hydration radii of Cl^- ions and large pore size distribution of the membrane. In this case, the separation mechanism of the

membranes was dominated by a collaborative effect of size-sieving and Donnan exclusion. Due to the negatively charged surface of the membrane, the Donnan repulsion effect for SO_4^{2-} ions was greater than that for Cl^- ions. As a result, high SO_4^{2-} rejection and low Cl^- rejection were obtained. Therefore, the membrane showed superior selectivity for mono- and divalent salts. From these studies, it is clear that the interlayer spacing of the membrane is important for high rejection and permeance. Therefore, modification of the material with a suitable cross-linking reagent is important to control the interlayer spacing of the membrane. In this regard, Jiang *et al.* cross-linked TaPa-SO_3 nanosheets with TpTTPA nanoribbons through electrostatic and pi-interactions to obtain a highly ordered and robust structural COF membrane.[124] This COF membrane showed 99.91% rejection of NaCl along with water permeance of 267 kg m^{-2} h^{-1}, which is 4 to 10 times higher than that of conventional membranes. These membranes showed superior operation stability for 108 h and good salinity tolerance (7.5%).

Molecular separations are processes that demand a lot of energy and can be employed in various separation industries.[125–128] The global shift towards sustainable production necessitates the development of novel, energy-efficient separation techniques. According to Livingston *et al.*,[129] the filtration processes can be categorized based on (i) the propelling force required for the separation; (ii) the size of the rejected solute or, in turn, the size of the pore; and (iii) the transport mechanism governing the separation. A separation membrane should have well-defined pore diameters so that it can maintain selectivity, be mechanically robust, and be as thin as feasible so that it can maximize the flow of solvent through it. On a molecular level, the interactions between solutes and membranes have a profound effect on separation behavior, based on the size, charge, hydrophilicity/hydrophobicity, and other physicochemical properties of the solute. It has been reported that 2D COFs with diverse types of planar organic building elements were used to construct a lamellar

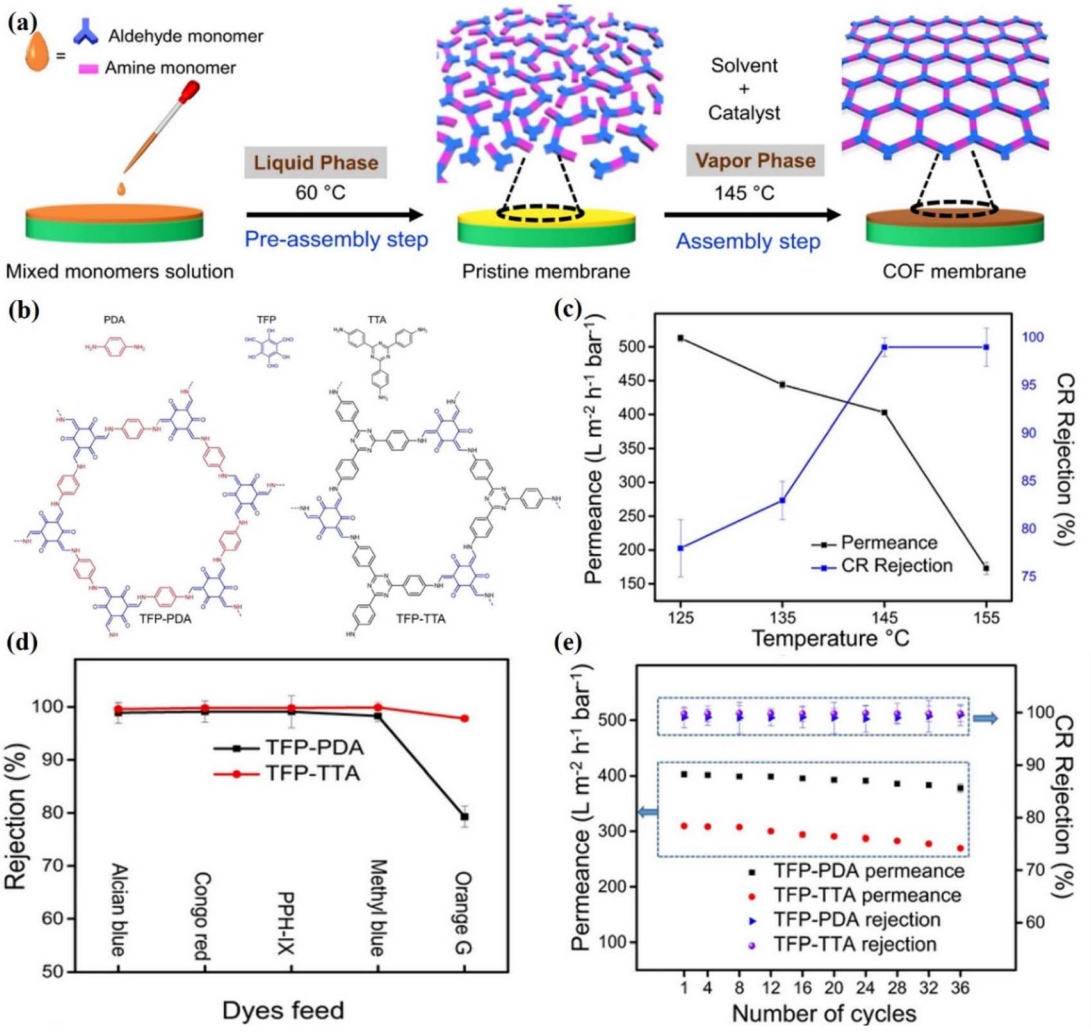

Fig. 10 (a) Fabrication of TFP-PDA and TFP-TTA COF membranes. A mixed monomer solution was cast on an ITO substrate in the pre-assembly step to obtain a pristine membrane at 60 °C, and subsequently the pristine membrane was heated at 145 °C in the assembly step to fabricate the COF membranes. (b) The chemical structure of both COF membranes. (c) Permeance and CR rejection of membranes fabricated at different temperatures after 18 h. (d) Separation efficiency for dyes. (e) The rejection and permeance of CR dye after a specified number of cycles. Data obtained with permission.[56] Copyright 2022, Springer Nature.

architecture.[116] Compared to GO membranes, 2D COF membranes have a high density of hydrophilic nanopores with a diameter of 2.8 nm and have superior water permeance up to 2260 L m^{-2} h^{-1} bar^{-1}. However, the molecular sieving effects are limited due to the larger pore size (0.8–4.7 nm) of COF membranes than the kinetic diameter of the majority of small molecules. Further, the weak interlamellar interaction between the COF nanosheets is responsible for insufficient mechanical strength of the membranes. Therefore, the fabrication of COF membranes by assembling 2D COF nanosheets is an extremely difficult process. Therefore, it is challenging to precisely tune the sub-nanometer pore size of COFs. A study showed that 1D cellulose nanofibers exhibit an abundance of functional groups like COFs.[48] Therefore, they bonded with each other through multiple interactions. The resulting shielding effect of cellulose nanofibers decreased the pore size of COF nanosheets and established a mechanically strong interlamellar microporous network. Therefore, these composite membranes showed high separation, such as 90.3%, 90.3%, 98.4% and 99.6% for orange GII (OG), methyl blue (MB), Alcian blue (AB), and congo red (CR), respectively. Shi *et al.* reported >99% rejection for AB, CR and MB molecules through imine-linked COF-based membranes.[76] These membranes exhibited 3 to 20 times higher water permeance with similar rejection. Lu *et al.* prepared novel polyamide membranes from amide-linked COFs with well-ordered pore structures.[130] These membranes exhibited not only high water permeability up to 482.3 L m^{-2} h^{-1} bar^{-1}, but also showed >99% rejection for methylene blue dye. In addition, these membranes have good stability under harsh environmental conditions. Zhang *et al.* reported a TpPA-wood membrane with a high separation efficiency of 97.0% for dyes and pharmaceutical molecules with a permeance of 600 L m^{-2} h^{-1}.[108] Additionally, this membrane is also stable at a broad pH range (3–11) and upon continuous filtration for 48 h. Khan *et al.* synthesized TFP-TTA and TFP-PDA COF membranes (Fig. 10a and b) at different temperatures ranging from 125 to 155 °C.[56] As shown in Fig. 10c, the TFP-PDA COF membrane prepared at 145 °C exhibited 99% rejection against CR dye along with permeance of 403 ± 4 L m^{-2} h^{-1} bar^{-1}. The authors also measured the water permeance of membranes assembled at different temperatures and showed water permeability of 513 ± 5, 444 ± 5, 403 ± 9, and 173 ± 9 L m^{-2} h^{-1} bar^{-1} at temperatures of 125 °C, 135 °C, and 155 °C, respectively. Results suggested that when the temperature increased from 125 °C to 155 °C, the CR rejection also increased from 78% to 99%. The low rejection rate of CR dye and high water permeance at 125 °C are due to low vapor pressure. Further, both membranes (TFP-PDA = 1.4 nm and TFP-TTA = 1.09 nm) were evaluated on the basis of their pore size. Therefore, different feed molecules with different sizes, such as AB (1.25 × 2.22 nm), PPH-IX (1.54 × 1.45 nm), CR (0.73 × 2.56 nm), MB dyes (1.74 × 2.36 nm) and OG (0.85 × 1.1 nm) were selected, as shown in Fig. 10d. Both membranes showed >98% rejection for larger feed molecules (AB, MB, CR, and PPH-IX). However due to the large pore size, the membranes showed less selectivity for small size molecules. In addition, the authors measured the stability of each membrane and found that both TFP-TTA COF and TFP-PA COF membranes are stable even after 96 h of continuous operation and retained a high water permeance (96.6% by TFP-TTA and 93.7% by TFP-PDA), as shown in Fig. 10e.

The pore size of the membrane is also essential for the rejection of small ions or molecules.[25] Therefore, the pore size of the COF membrane can be easily controlled by using polymers,[131–133] or 2D nanomaterials,[134–136] as cross-linkers. In addition, the doping of suitable functional materials,[137–142] or metal oxide nanoparticles,[143–148] can also tune the pore structure

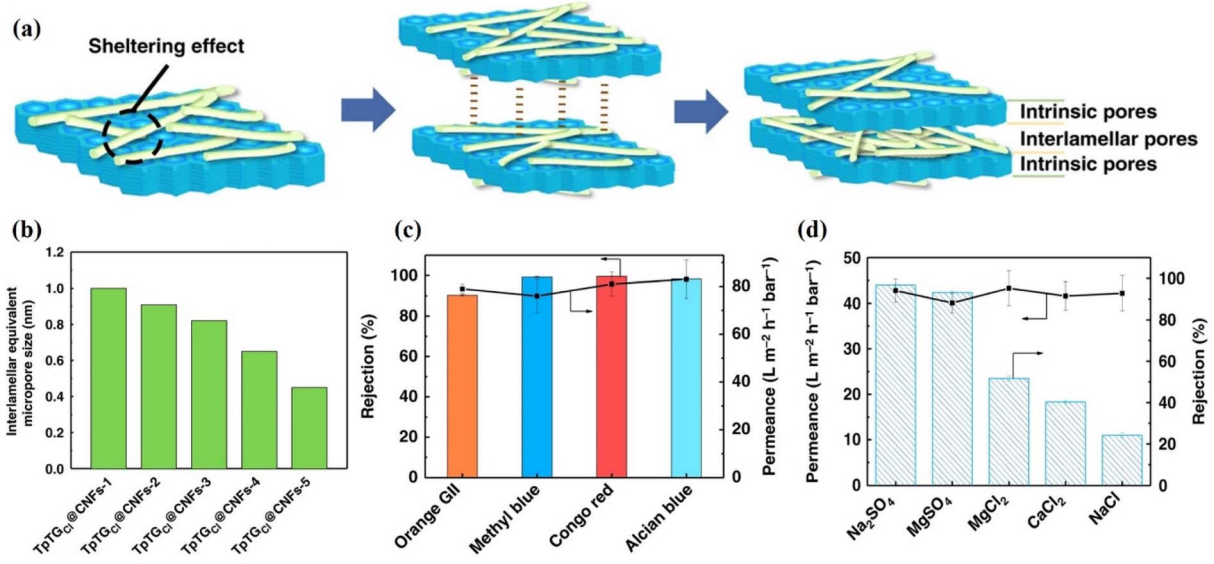

Fig. 11 (a–d) The TpTGCl@CNFs-3@PAN membranes. (a) A schematic depiction of the sheltering effect, interlamellar interactions, and pore structures. (b) The interlamellar equivalent pore size. (c and d) Separation performance against dyes (c) and salt (d) feed solution, respectively (100 ppm dye concentration and 0.2 MPa applied pressure were used for dye rejection, while the salt concentration used was 1000 ppm and applied pressure was 0.4 MPa). Data obtained with permission.[48] Copyright 2019, Springer Nature.

of the membrane. In this regard, Yang *et al.* modified a COF membrane with 1D cellulose fibers (CNFs) and controlled the pore size between 0.45 and 1.0 nm,[48] as depicted in Fig. 11a and b. Four different dye solutions (CR, AB, MB, and OG) with a concentration of 100 ppm were used to evaluate the rejection performance of the membranes (Fig. 11c). The TpTGCl@CNFs-3/PAN membrane showed rejection rates of 99.6%, 98.4%, 90.3%, and 90.3% for CR, AB, MB, and OG, respectively. The results indicated that if the size of the dye molecule is larger than 1 nm, then it is retained by the membrane with an interlamellar equivalent pore size of 0.82 nm, and shows permeance >70 L m^{-2} h^{-1} bar^{-1}. The CNF networks also influence the permeance of the membrane as well as its selectivity. The membrane with higher CNF quantity has a high dye rejection, while permeance decreases due to the dense CNF networks. Further, these membranes were also tested for measurement of salt rejection (Fig. 11d). The membrane with a pore size distribution of 0.65 nm exhibits a 96.8% rejection for Na_2SO_4 and permeance of 42.8 L m^{-2} h^{-1} bar^{-1}. Although the hydrated radii of all these ions, such as Na^+ (0.72 nm), Cl^- (0.66 nm), Ca^{2+} (0.82 nm), SO_4^{2-} (0.76 nm), and Mg^{2+} (0.86 nm), are larger than the pore size of the membrane (0.65 nm), the membrane still shows less rejection for $MgCl_2$, $CaCl_2$, and NaCl (Fig. 11d). This rejection mechanism could be explained by the synergistic Donnan exclusion and size sieving effect caused by charged functional groups on the membrane surface. The negatively charged membrane surface could attract cations, resulting in a concentration difference of ions in the solution and across the membrane, and a potential difference. The Donnan exclusion effect is more pronounced for sulfate salts than for chloride salts. Additionally, Cl^- has a smaller hydration radius (0.66 nm) than SO_4^{2-} (0.76 nm) ions. This Donnan exclusion, in conjunction with steric hindrance, results in a significant rejection for sulfate salts, while chloride salts experience a comparatively moderate rejection rate. Yang *et al.* used a 4-carboxyl-quinoline linked COF (QL-COF) membrane for rejection of different molecules.[149] The membrane exhibited high separation capacity (>90%) for vitamin B-12, RB, MB, CR, AF, chrome black T, AB, MLB, MO, and NR along with excellent water permeance of ~850 L m^{-2} h^{-1} MPa^{-1}. Corcos *et al.* used the IP method to probe 2D COFs, such as TAPB-PDA, TAPB-PDA-H and TAPB-Et and incorporated them into TFC on a PAN support.[150] All membranes showed the same topology throughout the series. The methyl and ethyl substitutes decreased the pore size of the membranes and increased efficiency against NaCl and rhodamine-WT solutions compared to the TAPB-PDA-H COF membrane. Besides these, several works have been published on the efficiency of COF membranes for rejection of organic pollutants.[59,72,111,151–153] He *et al.* used *in situ* homogenous polymerization to develop a chemically supported free-standing COF-TAPD film on a functionalized nylon support (COF-TAPD@nylon membrane).[154] The 22 μm-thick COF membrane showed high water permeance of ~2822 L m^{-2} h^{-1} MPa^{-1} and exhibited 99.8% rejection for CR dye. The membrane also showed high rejection of ~90.2% and ~85.6% for AB83 and MB dyes, respectively. The authors also reported 100% rejection for BSA feed solution through this membrane. The higher rejection of BSA is due to the large size of the molecule. Meanwhile, the COF-TAPD@nylon membrane with similar thickness showed almost no rejection for common salts such as NaCl, Na_2SO_4, and $CaCl_2$. This low rejection is due to the large pore size (~3.09 nm) of the membrane. In another study, an *in situ* IP method was used to prepare an ACOF-1/HPAN membrane.[54] The optimized membrane showed 99.2% rejection for CR and 96.6% rejection for MB dyes. Meanwhile, the membrane exhibited water permeance of ~142 L m^{-2} h^{-1} bar^{-1}, which is 5 to 12 times higher than that of reported membranes with similar rejections. Wang *et al.* reported high water permeance of ~380 L m^{-1} h^{-1} bar^{-1} through the TpEB-PAN membrane.[155] The authors used TpEB as a filler in the PAN membrane. The TpEB molecule increased water permeance to several times (35%) higher than that of the pure PAN membrane. The TpEB also increased the separation efficiency for BSA up to 92.6%. In addition, the TpEB-PAN membrane also has high operational stability and fouling resistivity.

4. Perspectives and future challenges

This review has shed light on COF-based laminates from both experimental and computational aspects. The material's structure, characteristics, synthesis, production processes, and prospective applications in ionic and molecular separation are highlighted. Based on the results of simulation, it appears that these membranes have superior separation in comparison to polymeric membranes. However, experimentally very little works has been published so far.

Separation of small ions and molecules is a great challenge for COF-based membranes due to their large interlayer spacing. Therefore, membranes must effectively manipulate pore aperture size at the subnanometer scale. In a few investigations, IP and polymer-assisted methods have been used to synthesize COF membranes for separation of small molecules. Due to their pore size (0.8 to 4.7 nm) being greater than the kinetic diameters of most nanoscale ions, including Na^+ (0.72 nm), Cl^- (0.66 nm), and SO_4^{2-} (0.76 nm), traditional COFs have poor ionic sieving effects. COF subnanometer pore diameters can be precisely adjusted through monomer design. In addition, the weak pi–pi interactions between COF nanocrystals reduced the mechanical strength of the membranes, causing severe defects. Therefore, it is highly desirable to design novel methods that can simultaneously change pore sizes for effective sieving, outstanding mechanical strength, superior separation performance, and enhanced stability of COF membranes.

Free-standing and mechanically robust COF-membranes are difficult to prepare. Researchers have mostly focused on the synthesis of self-supported COF membranes, which require a substantial thickness (typically hundreds of micrometers) to offer mechanical stability for large scale applications. Therefore, 2D COF has been deposited on porous substrates to prepare COF thin-film membranes with good mechanical strength. However, this technique causes structural instability and defects during the material's dispersion and needs harsh conditions like high temperatures and aggressive solvents. The poor interfacial adhesion between the COF layer and the

substrate greatly reduces the membrane's mechanical strength and operational endurance. In addition, the weak pi–pi interactions between COF nanocrystals are also responsible for the low mechanical strength of the membranes. Therefore, focus should be placed on self-supported COF-membranes and their testing under different pressures.

Theoretical studies suggested that mono-layered COF membranes have high separation performance. However, experimentally it is not easy to synthesize or transfer single-layered COF nanosheets with specific lateral dimensions onto porous substrates. Therefore, studies that bear close resemblance to real-world preparations and applications should also be done on single layer structures.

Cost-effective and efficient membranes for large-scale applications remain a formidable challenge for the scientific community. The high production cost of COFs limits their applications. However, newly developed technologies have reduced the price of COF nanomaterials to some extent. Methods to fabricate defect-free, larger area, 2D COFs with controllable pore structure/size and interlayer distance are being developed. Liquid phase methods, such as VF, require large volumes of liquid and more time, and are arguably hindered by alignment (of the GO sheets) and scalability problems. Other techniques, such as spin coating, dip-coating, drop casting, LbL assembly, *etc.*, may also experience problems with rapid production. The *in situ* growth method is most popular for fabrication of COF membranes. However, preparing a defect-free COF selective layer on a substratum *via* an *in situ* growth procedure at room temperature using environmentally friendly solvents remains a difficult challenge due to the rigid membrane formation conditions. This method only works for low viscous solvents. Consequently, for large-scale productivity and industrial use, novel fabrication methods that are cost-effective and save time are also required to maximize resource utilization. Developing a suitable substrate to prevent dispersion in the liquid phase and ensure water transport will undoubtedly be necessary.

2D COF membranes for water filtration have made great progress so far. But there is still a lot of work to be done. In reality, an ideal membrane is anticipated to be sufficiently robust to withstand the applied pressure and thin enough to have effective permeability. The ideal membranes for this application should have a high level of permeability and maximum rejection. The separation efficiency of the membrane is greatly impacted by the *d*-spacing and swelling effect, which must be controlled while improving ion permeability without compromising integrity, robustness in operation (high chemical, thermal, and mechanical stability), and other factors. Additionally, research on the antifouling properties of COF-based membranes has received less attention. Therefore, experimental study is needed in this direction.

Therefore, after removing these engineering hurdles, we expect 2D COF-based membranes to be used as next-generation water purification and desalination membranes. This may be possible with consistent effort, dedication, and multidisciplinary research.

Conflicts of interest

The authors declare no conflict of interest for this research work.

Acknowledgements

This work is supported by the Ministry of Science and Technology of China (No. 2016YFA0200101), National Science Foundation of China (No. 51325205, 51290273, and 51521091), and Chinese Academy of Sciences (KGZD-EW-303-1 and KGZD-EW-T06). We also thank the CAS-TWAS President Fellowship for the financial support and Government of Pakistan.

References

1 M. K. Shahzad, F. H. Memon, F. Soomro, M. Iqbal, A. Ibrar, A. A. Memon, J. H. Lim, K. H. Choi and K. H. Thebo, *J. Environ. Chem. Eng.*, 2023, **11**, 109329.
2 A. Ali, F. Rehman, M. Ali Khan, F. H. Memon, F. Soomro, M. Iqbal, J. Yang and K. H. Thebo, *ACS Omega*, 2022, **7**, 32410–32417.
3 B. Sun, Y. Kim, Y. Wang, H. Wang, J. Kim, X. Liu and M. Lee, *Nat. Mater.*, 2018, **17**, 599–604.
4 Y. Shao, M. F. El-Kady, L. J. Wang, Q. Zhang, Y. Li, H. Wang, M. F. Mousavi and R. B. Kaner, *Chem. Soc. Rev.*, 2015, **44**, 3639–3665.
5 H. W. Kim, H. W. Yoon, S.-M. Yoon, B. M. Yoo, B. K. Ahn, Y. H. Cho, H. J. Shin, H. Yang, U. Paik, S. Kwon, J.-Y. Choi and H. B. Park, *Science*, 2013, **342**, 91–95.
6 X. Qian, L. Chen, L. Yin, Z. Liu, S. Pei, F. Li, G. Hou, S. Chen, L. Song, K. H. Thebo, H.-M. Cheng and W. Ren, *Science*, 2020, **370**, 596–600.
7 S. Hussain, Y. Li, F. H. Memon, S. Hussain, L. Li and K. H. Thebo, *Prog. Nat. Sci.: Mater. Int.*, 2022, **32**, 128–134.
8 S. Hussain, Y. Li, A. Mustehsin, A. Ali, K. H. Thebo, Z. Ali and S. Hussain, *Ionics*, 2021, **27**, 4849–4857.
9 I. A. Soomro, F. H. Memon, W. Mughal, M. A. Khan, W. Ali, Y. Liu, K. H. Choi and K. H. Thebo, *Membranes*, 2023, **13**, 259.
10 R. Castro-Muñoz, *Water Res.*, 2020, **187**, 116428.
11 K. Banjerdteerakul, H. Peng and K. Li, *J. Membrane Sci.*, 2023, **678**, 121679.
12 D. Yang, C. Chen, J. Xie, Y. Ye, Z. Zhou, H. Liao and Z. Yao, *J. Environ. Chem. Eng.*, 2023, **11**, 109390.
13 M. Y. Jeon, D. Kim, P. Kumar, P. S. Lee, N. Rangnekar, P. Bai, M. Shete, B. Elyassi, H. S. Lee, K. Narasimharao, S. N. Basahel, S. Al-Thabaiti, W. Xu, H. J. Cho, E. O. Fetisov, R. Thyagarajan, R. F. DeJaco, W. Fan, K. A. Mkhoyan, J. I. Siepmann and M. Tsapatsis, *Nature*, 2017, **543**, 690.
14 W. Yuan, J. Chen and G. Shi, *Mater. Today*, 2014, **17**, 77–85.
15 M. Majumder, N. Chopra, R. Andrews and B. J. Hinds, *Nature*, 2005, **438**, 44.
16 Z. Ali, M. Mehmood, J. Ahmed, A. Majeed and K. H. Thebo, *Mater. Res. Express*, 2019, **6**, 105627.

17 Z. Ali, M. Mehmood, J. Ahmed, A. Majeed and K. H. Thebo, *Mater. Lett.*, 2020, **259**, 126831.
18 S. B. Jaffri, K. S. Ahmad, K. H. Thebo and F. Rehman, *Z. Phys. Chem.*, 2021, **235**, 1539–1572.
19 Z. Jiang, S. Karan and A. G. Livingston, *Adv. Mater.*, 2018, **30**, 1705973.
20 Z.-A. Qiao, S.-H. Chai, K. Nelson, Z. Bi, J. Chen, S. M. Mahurin, X. Zhu and S. Dai, *Nat. Commun.*, 2014, **5**, 3705.
21 R. K. Joshi, P. Carbone, F. C. Wang, V. G. Kravets, Y. Su, I. V. Grigorieva, H. A. Wu, A. K. Geim and R. R. Nair, *Science*, 2014, **343**, 752–754.
22 N. A. Nahyoon, L. Liu, K. Rabe, K. H. Thebo, L. Yuan, J. Sun and F. Yang, *Electrochim. Acta*, 2018, **271**, 41–48.
23 I. Chandio, F. A. Janjhi, A. A. Memon, S. Memon, Z. Ali, K. H. Thebo, A. A. A. Pirzado, A. A. Hakro and W. S. Khan, *Desalination*, 2021, **500**, 114848.
24 F. Ahmed Janjhi, I. Chandio, A. Ali Memon, Z. Ahmed, K. Hussain Thebo, A. Ali Ayaz Pirzado, A. Ali Hakro and M. Iqbal, *Sep. Purif. Technol.*, 2021, **274**, 117969.
25 A. Ali, M. Aamir, K. H. Thebo and J. Akhtar, *Chem. Rec.*, 2020, **20**, 344–354.
26 F. Rehman, K. H. Thebo, M. Aamir and J. Akhtar, in *Nanotechnology in the Beverage Industry*, eds., A. Amrane, S. Rajendran, T. A. Nguyen, A. A. Assadi and A. M. Sharoba, Elsevier, 2020, pp. 207–240.
27 D. Janwery, F. H. Memon, A. A. Memon, M. Iqbal, F. N. Memon, W. Ali, K.-H. Choi and K. H. Thebo, *ACS Omega*, 2023, **8**(8), 7648–7656.
28 Z. Yan, X. Liu, B. Ding, J. Yu and Y. Si, *Nat. Commun.*, 2023, **14**, 2116.
29 Y. Liu, Y. Liu, M. Chen, S. Liu, B. Lai and W. Tu, *J. Water Process. Eng.*, 2023, **51**, 103374.
30 B. Lal, K. B. Idrees, H. Xie, C. S. Smoljan, S. Shafaie, T. Islamoglu and O. K. Farha, *Angew. Chem., Int. Ed.*, 2023, **62**, e202219053.
31 W. Rahmah, G. T. M. Kadja, M. H. Mahyuddin, A. G. Saputro, H. K. Dipojono and I. G. Wenten, *J. Environ. Chem. Eng.*, 2022, **10**, 108707.
32 S.-L. Wee, C.-T. Tye and S. Bhatia, *Sep. Purif. Technol.*, 2008, **63**, 500–516.
33 C. Chen, J. Wang, D. Liu, C. Yang, Y. Liu, R. S. Ruoff and W. Lei, *Nat. Commun.*, 2018, **9**, 1902.
34 W. Lei, V. N. Mochalin, D. Liu, S. Qin, Y. Gogotsi and Y. Chen, *Nat. Commun.*, 2015, **6**, 8849.
35 F. A. Janjhi, I. Ihsanullah, M. Bilal, R. Castro-Muñoz, G. Boczkaj and F. Gallucci, *Water Resour. Ind.*, 2023, **29**, 100202.
36 Y. Gogotsi and B. Anasori, *ACS Nano*, 2019, **13**, 8491–8494.
37 M. Sajid, S. M. Sajid Jillani, N. Baig and K. Alhooshani, *Chemosphere*, 2022, **287**, 132140.
38 N. Baig, I. Kammakakam and W. Falath, *Mater. Adv.*, 2021, **2**, 1821–1871.
39 Y.-X. Sun, J. Zhao, X.-Z. Li, H. Jiang, Y.-J. Cai, X. Yang, Y. Liu, Y.-B. Li, Z.-H. Yang, Y.-G. Wu, L.-Y. Chen and J.-G. Gai, *ACS Appl. Mater. Interfaces*, 2023, **15**, 18550–18558.
40 X. Shi, Z. Zhang, S. Fang, J. Wang, Y. Zhang and Y. Wang, *Nano Lett.*, 2021, **21**, 8355–8362.
41 Z. Song, Q. Sun, J. Du, L. Liu, W. He, Y. Xu and J. Liu, *ACS Appl. Polymer Mater.*, 2023, **5**, 3043–3054.
42 X. You, L. Cao, Y. Liu, H. Wu, R. Li, Q. Xiao, J. Yuan, R. Zhang, C. Fan, X. Wang, P. Yang, X. Yang, Y. Ma and Z. Jiang, *ACS Nano*, 2022, **16**, 11781–11791.
43 L. Cao, I. C. Chen, Z. Li, X. Liu, M. Mubashir, R. A. Nuaimi and Z. Lai, *Nat. Commun.*, 2022, **13**, 7894.
44 A. P. Côté, A. I. Benin, N. W. Ockwig, M. O'Keeffe, A. J. Matzger and O. M. Yaghi, *Science*, 2005, **310**, 1166–1170.
45 G. Li, K. Zhang and T. Tsuru, *ACS Appl. Mater. Interfaces*, 2017, **9**, 8433–8436.
46 S. Zhao, C. Jiang, J. Fan, S. Hong, P. Mei, R. Yao, Y. Liu, S. Zhang, H. Li, H. Zhang, C. Sun, Z. Guo, P. Shao, Y. Zhu, J. Zhang, L. Guo, Y. Ma, J. Zhang, X. Feng, F. Wang, H. Wu and B. Wang, *Nat. Mater.*, 2021, **20**, 1551–1558.
47 W. Xian, X. Zuo, C. Zhu, Q. Guo, Q.-W. Meng, X. Zhu, S. Wang, S. Ma and Q. Sun, *Nat. Commun.*, 2022, **13**, 3386.
48 H. Yang, L. Yang, H. Wang, Z. Xu, Y. Zhao, Y. Luo, N. Nasir, Y. Song, H. Wu, F. Pan and Z. Jiang, *Nat. Commun.*, 2019, **10**, 2101.
49 S. Han, J. Zhu, A. A. Uliana, D. Li, Y. Zhang, L. Zhang, Y. Wang, T. He and M. Elimelech, *Nat. Commun.*, 2022, **13**, 7954.
50 R. K. Sharma, P. Yadav, M. Yadav, R. Gupta, P. Rana, A. Srivastava, R. Zbořil, R. S. Varma, M. Antonietti and M. B. Gawande, *Mater. Horiz.*, 2020, **7**, 411–454.
51 S. Karan, Z. Jiang and A. G. Livingston, *Science*, 2015, **348**, 1347–1351.
52 Z. Tan, S. Chen, X. Peng, L. Zhang and C. Gao, *Science*, 2018, **360**, 518–521.
53 N. A. Khan, H. Wu, Y. Jinqiu, W. Mengyuan, P. Yang, M. Long, A. U. Rahman, N. M. Ahmad, R. Zhang and Z. Jiang, *Sep. Purif. Technol.*, 2021, **274**, 119046.
54 D. Liu, K. Li, M. Li, Z. Wang, M. Shan and Y. Zhang, *ACS Appl. Mater. Interfaces*, 2021, **13**, 37775–37784.
55 M. Wu, J. Yuan, H. Wu, Y. Su, H. Yang, X. You, R. Zhang, X. He, N. A. Khan, R. Kasher and Z. Jiang, *J. Membrane Sci.*, 2019, **576**, 131–141.
56 N. A. Khan, R. Zhang, X. Wang, L. Cao, C. S. Azad, C. Fan, J. Yuan, M. Long, H. Wu, M. A. Olson and Z. Jiang, *Nat. Commun.*, 2022, **13**, 3169.
57 J. Liu, G. Han, D. Zhao, K. Lu, J. Gao and T.-S. Chung, *Sci. Adv.*, 2020, **6**, eabb1110.
58 M. Matsumoto, L. Valentino, G. M. Stiehl, H. B. Balch, A. R. Corcos, F. Wang, D. C. Ralph, B. J. Mariñas and W. R. Dichtel, *Chem*, 2018, **4**, 308–317.
59 D. B. Shinde, G. Sheng, X. Li, M. Ostwal, A.-H. Emwas, K.-W. Huang and Z. Lai, *J. Am. Chem. Soc.*, 2018, **140**, 14342–14349.
60 L. Valentino, M. Matsumoto, W. R. Dichtel and B. J. Mariñas, *Environ. Sci. Technol.*, 2017, **51**, 14352–14359.

61 K. Dey, M. Pal, K. C. Rout, S. Kunjattu H, A. Das, R. Mukherjee, U. K. Kharul and R. Banerjee, *J. Am. Chem. Soc.*, 2017, **139**, 13083–13091.
62 R. Wang, X. Shi, A. Xiao, W. Zhou and Y. Wang, *J. Membrane Sci.*, 2018, **566**, 197–204.
63 H. Wang, H. Wang, H. Jiang, A. Sheng, Z. Wei, Y. Li, C. Wu and H. Li, *ACS Appl. Nano Mater.*, 2020, **3**, 9329–9339.
64 Y.-Y. Su, X. Yan, Y. Chen, X.-J. Guo, X.-F. Chen and W.-Z. Lang, *J. Membrane Sci.*, 2021, **618**, 118706.
65 T. Wang, H. Wu, S. Zhao, W. Zhang, M. Tahir, Z. Wang and J. Wang, *Chem. Eng. J.*, 2020, **384**, 123347.
66 D. A. Dikin, S. Stankovich, E. J. Zimney, R. D. Piner, G. H. B. Dommett, G. Evmenenko, S. T. Nguyen and R. S. Ruoff, *Nature*, 2007, **448**, 457–460.
67 Y. Ying, D. Liu, J. Ma, M. Tong, W. Zhang, H. Huang, Q. Yang and C. Zhong, *J. Mater. Chem. A*, 2016, **4**, 13444–13449.
68 N. A. Khan, J. Yuan, H. Wu, L. Cao, R. Zhang, Y. Liu, L. Li, A. U. Rahman, R. Kasher and Z. Jiang, *ACS Appl. Mater. Interfaces*, 2019, **11**, 28978–28986.
69 H. Wang, Y. Zhai, Y. Li, Y. Cao, B. Shi, R. Li, Z. Zhu, H. Jiang, Z. Guo, M. Wang, L. Chen, Y. Liu, K.-G. Zhou, F. Pan and Z. Jiang, *Nat. Commun.*, 2022, **13**, 7123.
70 Y. Tang, S. Feng, L. Fan, J. Pang, W. Fan, G. Kong, Z. Kang and D. Sun, *Sep. Purif. Technol.*, 2019, **223**, 10–16.
71 F. Rehman, F. H. Memon, A. Ali, S. M. Khan, F. Soomro, M. Iqbal and K. H. Thebo, *Rev. Inorg. Chem.*, 2023, **43**, 13–31.
72 I. Gadwal, G. Sheng, R. L. Thankamony, Y. Liu, H. Li and Z. Lai, *ACS Appl. Mater. Interfaces*, 2018, **10**, 12295–12299.
73 D. D. Kulkarni, I. Choi, S. S. Singamaneni and V. V. Tsukruk, *ACS Nano*, 2010, **4**, 4667–4676.
74 Q. An, T. Huang and F. Shi, *Chem. Soc. Rev.*, 2018, **47**, 5061–5098.
75 Y. Ying, M. Tong, S. Ning, S. K. Ravi, S. B. Peh, S. C. Tan, S. J. Pennycook and D. Zhao, *J. Am. Chem. Soc.*, 2020, **142**, 4472–4480.
76 X. Shi, R. Wang, A. Xiao, T. Jia, S.-P. Sun and Y. Wang, *ACS Appl. Nano Mater.*, 2018, **1**, 6320–6326.
77 G. Liu, Z. Jiang, H. Yang, C. Li, H. Wang, M. Wang, Y. Song, H. Wu and F. Pan, *J. Membrane Sci.*, 2019, **572**, 557–566.
78 M. Fang, C. Montoro and M. Semsarilar, *Membranes*, 2020, **10**, 107.
79 S. Kandambeth, B. P. Biswal, H. D. Chaudhari, K. C. Rout, S. Kunjattu, S. Mitra, S. Karak, A. Das, R. Mukherjee, U. K. Kharul and R. Banerjee, *Adv. Mater.*, 2017, **29**, 1603945.
80 H. S. Sasmal, H. B. Aiyappa, S. N. Bhange, S. Karak, A. Halder, S. Kurungot and R. Banerjee, *Angew. Chem., Int. Ed.*, 2018, **57**, 10894–10898.
81 R. Wang, J. Guo, J. Xue and H. Wang, *Small Struct.*, 2021, **2**, 2100061.
82 A. Qadeer, Z. A. Saqib, Z. Ajmal, C. Xing, S. Khan Khalil, M. Usman, Y. Huang, S. Bashir, Z. Ahmad, S. Ahmed, K. H. Thebo and M. Liu, *Sustain. Cities Soc.*, 2020, **53**, 101959.
83 F. A. Janjhi, D. Janwery, I. Chandio, S. Ullah, F. Rehman, A. A. Memon, J. Hakami, F. Khan, G. Boczkaj and K. H. Thebo, *ChemBioEng Rev.*, 2022, **9**, 574–590.
84 I. Maqbool, F. Rehman, F. Soomro, Z. Bhatti, U. Ali, A. H. Jatoi, B. Lal, M. Iqbal, S. Phulpoto, A. Ali and K. H. Thebo, *ChemBioEng Rev.*, 2021, **8**, 67–77.
85 M. K. Shahzad, M. A. Khan, F. Soomro, Q.-U. Zaman, K. Sultan and K. H. Thebo, *Int. J. Environ. Anal. Chem.*, 2022, 1–14.
86 M.-U.-N. Khilji, N. A. Nahyoon, M. Mehdi, K. H. Thebo, N. Mahar, A. A. Memon, N. Memon and N. Hussain, *Opt. Mater.*, 2023, **135**, 113260.
87 S. A. Bhatti, F. H. Memon, F. Rehman, Z. Bhatti, T. Naqvi and K. H. Thebo, *Rev. Inorgan. Chem.*, 2022, **42**, 283–295.
88 M. Mehdi, W. Jiang, Q. Zeng, K. H. Thebo, I.-S. Kim, Z. Khatri, H. Wang, J. Hu and K.-Q. Zhang, *Langmuir*, 2022, **38**, 6376–6386.
89 A. A. Chandio, S. Memon, A. A. Memon, A. Balouch, R. Memon, K. H. Thebo, F. N. Memon, M. H. Agheem, S. S. Memon and A. A. Otho, *Polycyclic Aromat. Compd.*, 2023, **43**, 4843–4855.
90 K. H. Thebo, X. Qian, Q. Zhang, L. Chen, H. M. Cheng and W. Ren, *Nat. Commun.*, 2018, **9**, 1486.
91 Q. Zhang, X. Qian, K. H. Thebo, H.-M. Cheng and W. Ren, *Sci. Bull.*, 2018, **63**, 788–794.
92 A. Ali, R. Pothu, S. H. Siyal, S. Phulpoto, M. Sajjad and K. H. Thebo, *Mater. Sci. Energy Technol.*, 2019, **2**, 83–88.
93 K. H. Thebo, X. Qian, Q. Wei, Q. Zhang, H.-M. Cheng and W. Ren, *J. Mater. Sci. Technol.*, 2018, **34**, 1481–1486.
94 I. Mahar, F. H. Memon, J.-W. Lee, K. H. Kim, R. Ahmed, F. Soomro, F. Rehman, A. A. Memon, K. H. Thebo and K. H. Choi, *Membranes*, 2021, **11**, 869.
95 I. Mahar, F. K. Mahar, N. Mahar, A. A. Memon, A. A. A. Pirzado, Z. Khatri, K. H. Thebo and A. Ali, *Chem. Eng. Res. Des.*, 2023, **191**, 462–471.
96 Z. Ahmed, F. Rehman, U. Ali, A. Ali, M. Iqbal and K. H. Thebo, *ChemBioEng Rev.*, 2021, **8**, 110–120.
97 F. H. Memon, F. Rehman, J. Lee, F. Soomro, M. Iqbal, S. M. Khan, A. Ali, K. H. Thebo and K. H. Choi, *Sep. Purif. Rev.*, 2023, **52**, 43–57.
98 F. Rehman, F. Hussain Memon, S. Ullah, M. A. Jafar Mazumder, A. Al-Ahmed, F. Khan and K. Hussain Thebo, *Chem. Rec.*, 2022, **22**, e202200107.
99 S. Gao, Z. Li, Y. Yang, Z. Wang, Y. Wang, S. Luo, K. Yao, J. Qiu, H. Wang, L. Cao, Z. Lai and J. Wang, *ACS Appl. Mater. Interfaces*, 2021, **13**, 36507–36516.
100 Y. Zou, P. Wang, A. Zhang, Z. Qin, Y. Li, Y. Xianyu and H. Zhang, *ACS Appl. Mater. Interfaces*, 2022, **14**, 8680–8692.
101 M. Kato, R. Ota, T. Endo, T. Yanase, T. Nagahama and T. Shimada, *ACS Appl. Nano Mater.*, 2022, **5**, 2367–2374.
102 F. Ghanghermeh, F. Aghili and A. Rahimpour, in *Oil–Water Mixtures and Emulsions, Volume 2: Advanced Materials for Separation and Treatment*, American Chemical Society, 2022, vol. 1408, pp. 245–282.
103 W. Shi, C. Ye, X. Xu, X. Liu, M. Ding, W. Liu, X. Cao, J. Shen, H. Y. Yang and C. Gao, *ACS Omega*, 2018, **3**, 8506–8513.

104 A. A. Aslam, A. Irshad, M. S. Nazir and M. Atif, *J. Cleaner Prod.*, 2023, **400**, 136737.
105 Z. Zhang, A. Xiao, C. Yin, X. Wang, X. Shi and Y. Wang, *Chem. Commun.*, 2022, **58**, 7136–7139.
106 J. He, L. Yu, Z. Li, S. Ba, F. Lan and Y. Wu, *J. Colloid Interface Sci.*, 2023, **629**, 428–437.
107 Y. Lv, J. Ma, Z. Yu, S. Liu, G. Yang, Y. Liu, C. Lin, X. Ye, Y. Shi and M. Liu, *Water Res.*, 2023, **235**, 119892.
108 Z. Zhang, H. Li, J. Cui, Z. Yang, R. Hou, Y. Ju, X. Lu and F. Chen, *J. Cleaner Prod.*, 2023, **384**, 135595.
109 H. Ye, D. Chen, N. Li, Q. Xu, H. Li, J. He and J. Lu, *J. Membrane Sci.*, 2022, **655**, 120546.
110 Z. Li, Y. Zheng, T. Gu, X. Meng, H. Wang, K. Xu, L. Cheng, R. Kasher, R. Zhang and Z. Jiang, *J. Membrane Sci.*, 2023, **675**, 121551.
111 W. Zhou, M. Wei, X. Zhang, F. Xu and Y. Wang, *ACS Appl. Mater. Interfaces*, 2019, **11**, 16847–16854.
112 B. Niu, W. Xin, Y. Qian, X.-Y. Kong, L. Jiang and L. Wen, *Chem. Commun.*, 2022, **58**, 5403–5406.
113 S. Wang, L. Yang, K. Xu, H. Chen and N. Huang, *ACS Appl. Mater. Interfaces*, 2021, **13**, 44806–44813.
114 Q. Liang, B. Jiang, N. Yang, L. Zhang, Y. Sun and L. Zhang, *ACS Appl. Mater. Interfaces*, 2022, **14**, 45880–45892.
115 A. Chen, H. Guo, J. Zhou, Y. Li, X. He, L. Chen and Y. Zhang, *ACS Appl. Nano Mater.*, 2022, **5**, 3925–3936.
116 V. A. Kuehl, J. Yin, P. H. H. Duong, B. Mastorovich, B. Newell, K. D. Li-Oakey, B. A. Parkinson and J. O. Hoberg, *J. Am. Chem. Soc.*, 2018, **140**, 18200–18207.
117 F. Xu, M. Wei, X. Zhang and Y. Wang, *ACS Appl. Mater. Interfaces*, 2019, **11**, 45246–45255.
118 K. Zhang, Z. He, K. M. Gupta and J. Jiang, *Environ. Sci.: Water Res. Technol.*, 2017, **3**, 735–743.
119 F. Sheng, B. Wu, X. Li, T. Xu, M. A. Shehzad, X. Wang, L. Ge, H. Wang and T. Xu, *Adv. Mater.*, 2021, **33**, 2104404.
120 J. Shen, J. Yuan, B. Shi, X. You, R. Ding, T. Zhang, Y. Zhang, Y. Deng, J. Guan, M. Long, Y. Zheng, R. Zhang, H. Wu and Z. Jiang, *J. Mater. Chem. A*, 2021, **9**, 23178–23187.
121 H. Wang, J. Zhao, Y. Li, Y. Cao, Z. Zhu, M. Wang, R. Zhang, F. Pan and Z. Jiang, *Nano-Micro Lett.*, 2022, **14**, 216.
122 Y. Zheng, J. Shen, J. Yuan, N. A. Khan, X. You, C. Yang, S. Zhang, A. El-Gendi, H. Wu, R. Zhang and Z. Jiang, *Desalination*, 2022, **532**, 115753.
123 Y. Zhang, J. Guo, G. Han, Y. Bai, Q. Ge, J. Ma, C. H. Lau and L. Shao, *Sci. Adv.*, 2021, **7**, eabe8706.
124 M. Wang, P. Zhang, X. Liang, J. Zhao, Y. Liu, Y. Cao, H. Wang, Y. Chen, Z. Zhang, F. Pan, Z. Zhang and Z. Jiang, *Nat. Sustain.*, 2022, **5**, 518–526.
125 A. H. Jatoi, K. H. Kim, M. A. Khan, F. H. Memon, M. Iqbal, D. Janwery, S. N. Phulpoto, A. Samantasinghar, K. H. Choi and K. H. Thebo, *RSC Adv.*, 2023, **13**, 12695–12702.
126 F. Rehman, F. H. Memon, Z. Bhatti, M. Iqbal, F. Soomro, A. Ali and K. H. Thebo, *Rev. Inorgan. Chem.*, 2022, **42**, 327–336.
127 S. Sharif, K. S. Ahmad, F. H. Memon, F. Rehman, F. Soomro and K. H. Thebo, *Mater. Res. Innovations*, 2021, 1–9.
128 S. Sharif, K. S. Ahmad, F. Rehman, Z. Bhatti and K. H. Thebo, *J. Environ. Chem. Eng.*, 2021, **9**, 105605.
129 P. Marchetti, M. F. Jimenez Solomon, G. Szekely and A. G. Livingston, *Chem. Rev.*, 2014, **114**, 10735–10806.
130 Y. Lu, Z.-B. Zhou, Q.-Y. Qi, J. Yao and X. Zhao, *ACS Appl. Mater. Interfaces*, 2022, **14**, 37019–37027.
131 G. Liu, L. Cheng, G. Chen, F. Liang, G. Liu and W. Jin, *Chem.–Asian. J.*, 2020, **15**, 2364–2370.
132 M. Kaleem Shabbir, A. S. Syed and J. Akhtar, in *Smart Multifunctional Nano-inks*, eds., R. K. Gupta and T. A. Nguyen, Elsevier, 2023, pp. 429–449.
133 Y. Fang, X. J. Huang, P. C. Chen and Z. K. Xu, *BMB Rep.*, 2011, **44**, 87–95.
134 Z. Lu, Y. Wei, J. Deng, L. Ding and Z. Li, *ACS Nano*, 2019, **13**(9), 10535–10544.
135 L. Li, Y. Yu, G. J. Ye, Q. Ge, X. Ou, H. Wu, D. Feng, X. H. Chen and Y. Zhang, *Nat. Nanotechnol.*, 2014, **9**, 372–377.
136 R. Cao, H. Ding, K.-J. Kim, Z. Peng, J. Wu, J. T. Culp, P. R. Ohodnicki, E. Beckman and K. P. Chen, *Sens. Actuators, B*, 2020, **324**, 128627.
137 F. Soomro, J. Khan, S. Ullah, A. Abutaleb, N. Zouli, M. Iqbal, M. Sajjad, F. Khan and K. HussainThebo, *Inorg. Chem. Commun.*, 2023, **155**, 111023.
138 J. Khan, H. Ullah, M. Sajjad, W. B. Jatoi, A. Ali, K. Khan and K. H. Thebo, *Mater. Res. Express*, 2019, **6**, 075074.
139 J. Khan, H. Ullah, M. Sajjad, A. Bahadar, Z. Bhatti, F. Soomro, F. Hussain Memon, M. Iqbal, F. Rehman and K. Hussain Thebo, *Inorg. Chem. Commun.*, 2021, **130**, 108751.
140 J. Khan, H. Ullah, M. Sajjad, A. Ali and K. H. Thebo, *Inorg. Chem. Commun.*, 2018, **98**, 132–140.
141 S. Hussain, Y. Li, K. H. Thebo, Z. Ali, M. Owais and S. Hussain, *Mater. Chem. Phys.*, 2021, **267**, 124576.
142 K. Khan, A. K. Tareen, M. Aslam, K. H. Thebo, U. Khan, R. Wang, S. S. Shams, Z. Han and Z. Ouyang, *Prog. Solid State Chem.*, 2019, **54**, 1–19.
143 M. Iqbal, A. A. Thebo, W. B. Jatoi, M. T. Tabassum, M. U. Rehman, K. H. Thebo, M. A. Mohsin, S. Ullah, A. H. Jatoi and I. Shah, *Inorg. Chem. Commun.*, 2020, **116**, 107902.
144 M. Iqbal, A. A. Thebo, A. H. Shah, A. Iqbal, K. H. Thebo, S. Phulpoto and M. A. Mohsin, *Inorg. Chem. Commun.*, 2017, **76**, 71–76.
145 M. Iqbal, A. Ibrar, A. Ali, F. H. Memon, F. Rehman, Z. Bhatti, F. Soomro, A. Ali and K. H. Thebo, *Int. Nano Lett.*, 2022, **12**, 205–213.
146 M. Iqbal, A. Ibrar, A. Ali, S. Hussain, S. Shad, S. Ullah, T. Alshahrani, J. Hakami, F. Khan and K. H. Thebo, *J. Mol. Struct.*, 2022, **1267**, 133598.
147 M. Iqbal, A. Ali, N. A. Nahyoon, A. Majeed, R. Pothu, S. Phulpoto and K. H. Thebo, *Mater. Sci. Energy Technol.*, 2019, **2**, 41–45.
148 M. Iqbal, A. Ali, K. S. Ahmad, F. M. Rana, J. Khan, K. Khan and K. H. Thebo, *SN Appl. Sci.*, 2019, **1**, 647.
149 Y. Yang, L. Yu, T. Chu, H. Niu, J. Wang and Y. Cai, *Nat. Commun.*, 2022, **13**, 2615.

150 A. R. Corcos, G. A. Levato, Z. Jiang, A. M. Evans, A. G. Livingston, B. J. Mariñas and W. R. Dichtel, *ACS Mater. Lett.*, 2019, **1**, 440–446.
151 H. Fan, J. Gu, H. Meng, A. Knebel and J. Caro, *Angew. Chem., Int. Ed.*, 2018, **57**, 4083–4087.
152 W. Zhang, L. Zhang, H. Zhao, B. Li and H. Ma, *J. Mater. Chem. A*, 2018, **6**, 13331–13339.
153 Q. Hao, C. Zhao, B. Sun, C. Lu, J. Liu, M. Liu, L.-J. Wan and D. Wang, *J. Am. Chem. Soc.*, 2018, **140**, 12152–12158.
154 Y. He, X. Lin, J. Chen and Z. Guo, *ACS Appl. Mater. Interfaces*, 2020, **12**, 41942–41949.
155 X. Wang, X. Shi and Y. Wang, *Langmuir*, 2020, **36**, 10970–10978.
156 S. Hao, T. Zhang, S. Fan, Z. Jia and Y. Yang, *Chem. Eng. J.*, 2021, **421**, 129750.
157 C. Yin, S. Fang, X. Shi, Z. Zhang and Y. Wang, *J. Membrane Sci.*, 2021, **618**, 118727.
158 P. H. H. Duong, V. A. Kuehl, B. Mastorovich, J. O. Hoberg, B. A. Parkinson and K. D. Li-Oakey, *J. Membrane Sci.*, 2019, **574**, 338–348.
159 L. Xu, J. Xu, B. Shan, X. Wang and C. Gao, *J. Membrane Sci.*, 2017, **526**, 355–366.
160 A. Halder, S. Karak, M. Addicoat, S. Bera, A. Chakraborty, S. H. Kunjattu, P. Pachfule, T. Heine and R. Banerjee, *Angew. Chem., Int. Ed.*, 2018, **57**, 5797–5802.
161 J. Li, H. Rong, Y. Chen, H. Zhang, T. X. Liu, Y. Yuan, X. Zou and G. Zhu, *Chem. Commun.*, 2020, **56**, 6519–6522.
162 N. A. Khan, R. Zhang, H. Wu, J. Shen, J. Yuan, C. Fan, L. Cao, M. A. Olson and Z. Jiang, *J. Am. Chem. Soc.*, 2020, **142**, 13450–13458.
163 X. Shi, A. Xiao, C. Zhang and Y. Wang, *J. Membrane Sci.*, 2019, **576**, 116–122.
164 C. Liu, Y. Jiang, A. Nalaparaju, J. Jiang and A. Huang, *J. Mater. Chem. A*, 2019, **7**, 24205–24210.
165 A. Xiao, Z. Zhang, X. Shi and Y. Wang, *ACS Appl. Mater. Interfaces*, 2019, **11**, 44783–44791.
166 Z. Wang, Z. Si, D. Cai, G. L. Shufeng Li and P. Qin, *J. Membrane Sci.*, 2020, **615**, 118466.
167 A. Xiao, X. Shi, Z. Zhang, C. Yin, S. Xiong and Y. Wang, *J. Membrane Sci.*, 2021, **624**, 119122.
168 C. Wu, X. Wang, T. Zhu, P. Li and S. Xia, *Chemosphere*, 2020, **261**, 127580.
169 Y. Qu, Y. Zha, X. Du, S. Xu, M. Zhang, L. Xu and H. Jia, *ACS Appl. Polymer Mater.*, 2022, **4**, 7528–7536.
170 L. Chen, W. Wang, Q. Fang, K. Zuo, G. Hou, Q. Ai, Q. Li, L. Ci and J. Lou, *Appl. Mater. Today*, 2020, **20**, 100791.
171 G. Kong, J. Pang, Y. Tang, L. Fan, H. Sun, R. Wang, S. Feng, Y. Feng, W. Fan, W. Kang, H. Guo, Z. Kang and D. Sun, *J. Mater. Chem. A*, 2019, **7**, 24301–24310.
172 F. Pan, W. Guo, Y. Su, N. A. Khan, H. Yang and Z. Jiang, *Sep. Purif. Technol.*, 2019, **215**, 582–589.
173 J. Shen, R. Zhang, Y. Su, B. Shi, X. You, W. Guo, Y. Ma, J. Yuan, F. Wang and Z. Jiang, *J. Mater. Chem. A*, 2019, **7**, 18063–18071.
174 R. Wang, X. Shi, Z. Zhang, A. Xiao, S.-P. Sun, Z. Cui and Y. Wang, *J. Membrane Sci.*, 2019, **586**, 274–280.
175 X. Zhang, H. Li, J. Wang, D. Peng, J. Liu and Y. Zhang, *J. Membrane Sci.*, 2019, **581**, 321–330.
176 X. Sui, Z. Yuan, C. Liu, L. Wei, M. Xu, F. Liu, A. Montoya, K. Goh and Y. Chen, *J. Mater. Chem. A*, 2020, **8**, 9713–9725.
177 M. Wang, W. Guo, Z. Jiang and F. Pan, *Chin. J. Chem. Eng.*, 2020, **28**, 1039–1045.
178 J. Yao, C. Liu, X. Liu, J. Guo, S. Zhang, J. Zheng and S. Li, *J. Membrane Sci.*, 2020, **601**, 117864.
179 C. Yin, Z. Zhang, J. Zhou and Y. Wang, *ACS Appl. Mater. Interfaces*, 2020, **12**, 18944–18951.
180 T. Chen, B. Li, W. Huang, C. Lin, G. Li, H. Ren, Y. Wu, S. Chen, W. Zhang and H. Ma, *Sep. Purif. Technol.*, 2021, **256**, 117787.
181 Y. Li, M. Zhang, X. Guo, R. Wen, X. Li, X. Li, S. Li and L. Ma, *Nanoscale Horiz.*, 2018, **3**, 205–212.
182 J. Yuan, M. Wu, H. Wu, Y. Liu, X. You, R. Zhang, Y. Su, H. Yang, J. Shen and Z. Jiang, *J. Mater. Chem. A*, 2019, **7**, 25641–25649.
183 Z. Zhang, X. Shi, R. Wang, A. Xiao and Y. Wang, *Chem. Sci.*, 2019, **10**, 9077–9083.
184 N. A. Khan, J. Yuan, H. Wu, T. Huang, X. You, A. U. Rahman, C. S. Azad, M. A. Olson and Z. Jiang, *ACS Appl. Mater. Interfaces*, 2020, **12**, 27777–27785.
185 C. Li, S. Li, J. Zhang, C. Yang, B. Su, L. Han and X. Gao, *J. Membrane Sci.*, 2020, **604**, 118065.
186 R. Wang, M. Wei and Y. Wang, *J. Membrane Sci.*, 2020, **604**, 118090.
187 L. Xu, B. Shan, C. Gao and J. Xu, *J. Membrane Sci.*, 2020, **593**, 117398.
188 L. Xu, T. Yang, M. Li, J. Chang and J. Xu, *J. Membrane Sci.*, 2020, **610**, 118111.
189 Z. Zhang, C. Yin, G. Yang, A. Xiao, X. Shi, W. Xing and Y. Wang, *J. Membrane Sci.*, 2021, **618**, 118754.
190 F.-x. Kong, L. Yue, Z. Yang, G. Sun and J.-f. Chen, *ACS Appl. Mater. Interfaces*, 2021, **13**, 21379–21389.
191 C. Li, S. Li, L. Tian, J. Zhang, B. Su and M. Z. Hu, *J. Membrane Sci.*, 2019, **572**, 520–531.
192 S. Hao, L. Jiang, Y. L. Li, Z. Q. Jia and B. Van der Bruggen, *Chem. Commun.*, 2020, **56**, 419.
193 Y. S. He, X. G. Lin, J. H. Chen, Z. Y. Guo and H. B. Zhan, *ACS Appl. Mater. Interfaces*, 2020, **12**, 41942.